5-16-2022

Murphy Scale: A Locational Equivalent Intensity Scale for Hazard Events

Yi Victor Wang
Chapman University, ywang2@chapman.edu

Antonia Sebastian
University of North Carolina at Chapel Hill

Recommended Citation

Wang, Y. V., & Sebastian, A. (2022). Murphy Scale: A locational equivalent intensity scale for hazard events. *Risk Analysis*, 1–19. https://doi.org/10.1111/risa.13933

Murphy Scale: A Locational Equivalent Intensity Scale for Hazard Events

DOI: 10.1111/risa.13933

ORIGINAL ARTICLE

Murphy Scale: A locational equivalent intensity scale for hazard events

Yi Victor Wang[1] | **Antonia Sebastian**[2]

[1]Institute for Earth, Computing, Human and Observing (ECHO), Chapman University, Orange, California, USA

[2]Department of Earth, Marine and Environmental Sciences, University of North Carolina at Chapel Hill, Chapel Hill, North Carolina, USA

Correspondence
Yi Victor Wang, Institute for ECHO, Chapman University, One University Drive, Orange, CA 92866, USA.
Email: ywang2@chapman.edu

Abstract

Empirical cross-hazard analysis and prediction of disaster vulnerability, resilience, and risk requires a common metric of hazard strengths across hazard types. In this paper, the authors propose an *equivalent intensity scale* for cross-hazard evaluation of hazard strengths of events for entire durations at locations. The proposed scale is called the *Murphy Scale*, after Professor Colleen Murphy. A systematic review and typology of hazard strength metrics is presented to facilitate the delineation of the defining dimensions of the proposed scale. An empirical methodology is introduced to derive equivalent intensities of hazard events on a Murphy Scale. Using historical data on impacts and hazard strength indicators of events from 2013 to 2017, the authors demonstrate the utility of the proposed methodology for computing the equivalent intensities for earthquakes and tropical cyclones. As part of a new area of research called *hazard equivalency*, the proposed Murphy Scale paves the way toward creating multi-hazard hazard maps. The proposed scale can also be leveraged to facilitate hazard communication regarding past and future local experiences of hazard events for enhancing multi-hazard preparedness, mitigation, and emergency response.

KEYWORDS

global disaster research, hazard equivalency, hazard intensity, hazard strength, multi-hazard

1 | INTRODUCTION

With growing amounts of historical data on hazard impacts, empirical risk analysis has become increasingly important in disaster risk reduction (see, e.g., Bakkensen et al., 2016; Formetta & Feyen, 2019; Lin et al., 2017; H. Wang, 2020; Wang & Sebastian, 2021a; Wang et al., 2021). An empirical disaster risk analysis usually involves evaluation of expectations of frequencies of hazard events with measures of hazard strengths, exposed values of entities of interest, and vulnerability of entities exposed to hazard events (Cutter, 1996; Wang & Sebastian, 2021a; Wang et al., 2021; Wisner et al., 2004). A *hazard event* is a process (Wang et al., 2021), confined in space and time, that may result in negative consequences due to a set of hazard elements such as ground movement (Wang et al., 2019), storm surge (Bass et al., 2018), moisture deprivation (Zeff et al., 2020), wind gust (Lombardo & Ayyub, 2015), temperature extremization (Shafiei Shiva et al., 2019), meteoroid airburst (Y. V. Wang, 2020), disease spread (Gatto et al., 2020), or radiation leak (Wheatley et al., 2017). To reduce the negative consequences of hazards, it is essential that professionals are able to manage past and future hazard events across hazard types within their jurisdictions (Bodas et al., 2020). For such a purpose, a multi-hazard approach is usually recommended to assess preevent vulnerability and exposure to facilitate decision making regarding emergency preparedness, response, recovery, and mitigation (Ahmed & Kelman, 2018; Birkmann, 2013; Cutter, 1996; Cutter et al., 2000; Gautam, 2017; McEntire, 2012; Morrow, 1999; Pelling, 2003; Ribot, 2014; Rivera & Kapucu, 2015; Sutley et al., 2017; Tate, 2012; Turner et al., 2003; Wisner et al., 2004). However, current attempts with such a multi-hazard approach are limited because they lack objective computational methodology for

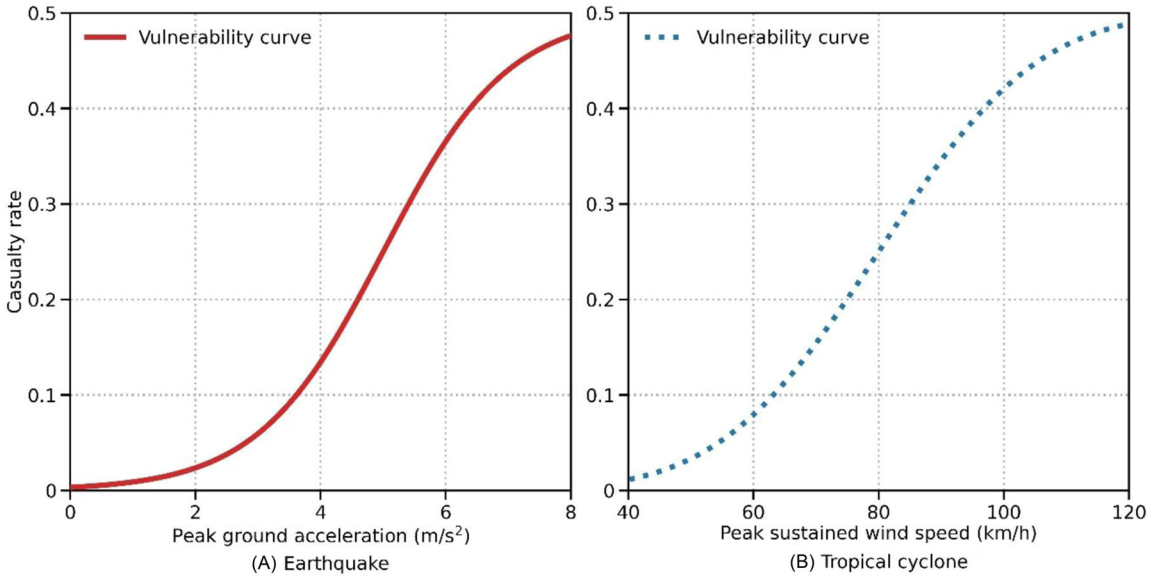

FIGURE 1 Illustrative examples of community vulnerability to hazard events in terms of the expected casualty rate with respect to a spectrum of (A) peak ground acceleration for earthquake and (B) peak sustained wind speed for tropical cyclone

comparative evaluation of hazard strengths across hazard types. Each community faces a different portfolio of hazards. Without fair benchmark measures of hazard strengths across hazard types, analyses of vulnerability, resilience, and risk for different communities are inevitably inaccurate within a multi-hazard context. Such inaccurate analyses will lead to unfair allocations of resources for disaster management and may result in inequitable impacts when severe hazard events do occur.

As an example, for computing risk as the expectation of losses due to future hazard events, quantitative modelers have recently proposed frameworks based on empirical predictive modeling approaches to quantify vulnerability of communities to hazard events (e.g., Wang & Sebastian, 2021a; Wang et al., 2019, 2020, 2021). For each individual hazard type, as shown in Figure 1, vulnerability can be modeled with a vulnerability curve representing a loss ratio, such as casualty rate, as a function of a hazard strength indicator. Such a hazard strength indicator can be peak ground acceleration (PGA) for earthquake (Figure 1A) or peak sustained wind speed (PSWS) for tropical cyclone (Figure 1B). However, without a common scale to represent the hazard strength indicator (on the horizontal axes of Figures 1A and B), it is difficult to evaluate vulnerability of communities to hazard events across hazard types.

To enable cross-hazard quantification and comparison of disaster vulnerability, resilience, and risk with respect to the entire durations of hazard events at locations, the authors propose an *equivalent intensity scale*—the *Murphy Scale*—and a data-driven methodology to derive the equivalent intensities of hazard events on the Murphy Scale. The proposed scale is named after the Roger and Stephany Joslin Professor of Law and Professor of Philosophy and Political Science Colleen Murphy at the University of Illinois at Urbana–Champaign (see Murphy, 2010, 2017, 2020a, 2020b; Murphy & Gardoni, 2006, 2008, 2010, 2011). The Murphy Scale is proposed to refer to *the locational-durational hazard strength scale for multiple types of hazards*. This definition will be explained in Section 2.

There are four main sections in this article. We first review the existing hazard strength scales with a proposal of typology on hazard strength metrics based on four dimensions and explain the definition of the proposed Murphy Scale. We then introduce the data-driven methodology to derive the equivalent intensities for hazard events on a Murphy Scale. Next, as a demonstrative example, we implement a Bayesian binomial regression approach with historical data on damages associated with 937 earthquakes and 320 tropical cyclones across the world from 2013 to 2017 to derive a prototype version of Murphy Scale for earthquake and tropical cyclone. Lastly, we discuss potential applications of Murphy Scale, relationship between a Murphy Scale and singular hazard strength scales, future improvement of formulation of Murphy Scale, and requirements for data collection for the development of Murphy Scale.

2 | HAZARD STRENGTH SCALES

In this article, we use the term *hazard strength scale* to refer to a metric indicating the size or severity of a hazard event, given an average exposed value and vulnerability of entities of interest that may be affected by the hazard event. Such a metric is usually called hazard magnitude or intensity (Alexander, 2018; Blong, 2003). Apart from few works (e.g., Kappes et al., 2012; Loat, 2010, Wang & Sebastian, 2021b), most of the existing hazard strength scales have been developed for a specific type of hazard event such as an

earthquake, tropical cyclone, drought, or nuclear accident. We call such a hazard event a *singular hazard event*, even though it may be associated with multiple hazard elements, including, for example, ground shaking, building collapse, liquefaction, and rockfall for an earthquake and wind gust, storm surge, and riverine flood for a tropical cyclone. Accordingly, we use the term *singular hazard strength scale* to refer to the hazard strength scale for a singular hazard event.

Since there were limited scholarly efforts on generalization of properties of hazard strength scales across hazard types, we conducted a literature review and examined 69 existing hazard strength scales for 21 singular hazard types as well as for multiple hazards, as summarized in Table 1. Based on this literature review, we suggested four dimensions for classification of hazard strength scales. These four dimensions include the spatial, temporal, applicational, and indicial dimensions. We will elaborate on these four dimensions in the following subsections. With the introduction of the four dimensions of hazard strength scales, we will be able to delineate the definition of the proposed Murphy Scale.

2.1 | Four dimensions of hazard strength scales

Among the four suggested dimensions of hazard strength scales, the spatial and temporal dimensions provide the defining criteria for classifying hazard strength scales. Meanwhile, the other two dimensions, that is, the applicational and indicial dimensions, are of practical significance when the corresponding hazard strength scales are derived and presented, for example, in communications to the public. All four dimensions of hazard strength scales can also be used to categorize hazard strength indicators of hazard events.

2.1.1 | Spatial dimension

The spatial dimension describes whether a hazard strength scale refers to the entire space occupied by the agent (for meaning of agent, see, e.g., Lindell & Prater, 2003; McEntire et al., 2002; Mileti & Peek, 2000; Quarantelli, 1984; Rodríguez et al., 2007) of a hazard event or specific locations at which entities of interest experience the hazard event. If a scale is for the entire space of the agent, we call it an *agential scale*, whereas a location-specific scale is called a *locational scale*. For example, in the case of earthquakes, the magnitude scales such as the Richter magnitude (Richter, 1935) and moment magnitude (Kanamori, 1977) correspond to a logarithmic representation of the energy released by the source of an earthquake event. Therefore, these earthquake magnitude scales are agential scales. Meanwhile, the earthquake intensity scales such as the modified Mercalli intensity (Wald et al., 2006; Wood & Neumann, 1931) and Shindo (Japan Meteorological Agency, 2019) are locational scales, because the earthquake intensity measures on these intensity scales indicate the severity of earthquake ground shaking at specific locations. Values on a locational scale across the entire spatial range of a hazard event may be aggregated to derive a single value for the purpose of an agential scale. As an example, values of the enhanced Fujita scale (Potter, 2007) for a tornado are determined locationally based on local observations of environmental damages. The maximum value on the enhanced Fujita scale (Potter, 2007) for the tornado can then be derived and assigned to the tornado event as a proxy on an agential scale.

A locational scale is usually adopted to correspond to a two-dimensional space. Within this two-dimensional space, a locational scale may have different levels of resolution. It may be associated with hazard strength measures at gauge stations as point locations, at grid cells with a unit size, or at administrative areas with different spatial sizes. Despite its popular utility for two-dimensional hazard modeling, a locational scale may also be adopted to indicate the local severity of a hazard event in a one-dimensional or three-dimensional space or for a network with a fractal dimension.

2.1.2 | Temporal dimension

The temporal dimension presents if a hazard strength scale corresponds to the entire duration of a hazard event or specific moments at which the event is experienced by entities of interest. A scale for the entire duration of a hazard event is called a *durational scale*. Meanwhile, if a scale is for moments, we call it a *momental scale*. A momental scale is usually presented with a certain temporal resolution in seconds, minutes, hours, days, weeks, months, or years. For hazard types whose events are with short durations, their corresponding hazard strength scales are usually durational. For example, the reviewed hazard strength scales of short-duration hazard events such as earthquakes (Grünthal, 1998; Japan Meteorological Agency, 2019; Kanamori, 1977; Katsumata, 1996; Liu et al., 2006; Rautian et al., 2007; Richter, 1935; Serva et al., 2016; Wald et al., 2006; Wood & Neumann, 1931), landslides (Arbanas & Arbanas, 2015; Hungr, 2018; Singh et al., 2019; Tanyaş et al., 2018), ice storms (spia-index.com, 2019), hailstorms (The Tornado and Storm Research Organisation, 2021), and explosions (Maienschein, 2002) are all durational scales (Table 1). In addition, for some hazard events, such as tropical cyclones, with possibly relatively long durations, both durational and momental scales may be developed for different purposes (Bell et al., 2000; Bloemendaal et al., 2021; Bureau of Meteorology, 2019; Emanuel, 2005; Hebert et al., 2010; National Disaster Management Authority, 2008; National Hurricane Center & Central Pacific Hurricane Center, 2019; Powell & Reinhold, 2007; Simpson & Saffir, 1974; Typhoon Committee, 2018; World Meteorological Organization, 2016). For tropical cyclones, for example, the accumulated cyclone energy index (Bell et al., 2000) is a durational scale to refer to the level of total energy of a hurricane during its lifespan. In the meantime, the Saffir–Simpson hurricane wind scale (National Hurricane Center & Central Pacific

TABLE 1 Examples of hazard strength scales

Hazard	Scale	Spatial dimension	Temporal dimension	Applicational dimension	Indicial dimension
Earthquake	Richter magnitude (Richter, 1935)	Agential	Durational	Numerical	Processual
	Surface wave magnitude (Liu et al., 2006)	Agential	Durational	Numerical	Processual
	Japan Meteorological Agency magnitude (Katsumata, 1996)	Agential	Durational	Numerical	Processual
	Moment magnitude (Kanamori, 1977)	Agential	Durational	Numerical	Processual
	Energy class scale (Rautian et al., 2007)	Agential	Durational	Numerical	Processual
	Environmental seismic intensity scale (Serva et al., 2016)	Locational	Durational	Ordinal	Processual
	European macroseismic scale (Grünthal, 1998)	Locational	Durational	Ordinal	Consequential
	Modified Mercalli intensity scale (Wald et al., 2006; Wood & Neumann, 1931)	Locational	Durational	Ordinal	Consequential or processual
	Shindo (Japan Meteorological Agency, 2019)	Locational	Durational	Ordinal	Consequential
Tsunami	Murty–Loomis magnitude scale (Murty & Loomis, 1980)	Agential	Durational	Numerical	Processual
	Abe scale (Abe, 1979)	Agential	Durational	Numerical	Processual
	Sieberg–Ambraseys intensity scale (Ambraseys, 1962)	Locational	Durational	Ordinal	Consequential and processual
	Imamura–Iida intensity scale (Shuto, 1993)	Locational	Durational	Numerical	Processual
	Integrated tsunami intensity scale (Lekkas et al., 2013)	Locational	Durational	Ordinal	Consequential and processual
Landslide	Landslide magnitude (Arbanas & Arbanas, 2015)	Agential	Durational	Numerical	Processual
	Earthquake-triggered landslide magnitude (Tanyaş et al., 2018)	Agential	Durational	Numerical	Processual
	Landslide intensity (Hungr, 2018; Singh et al., 2019)	Locational	Durational	Numerical	Processual
Volcanic activity	Dispersal index (Walker, 1973)	Agential	Durational	Numerical	Processual
	Volcanic explosivity index (Newhall & Self, 1982)	Agential	Durational	Ordinal	Processual
	Pyle magnitude (Pyle, 1995)	Agential	Durational	Numerical	Processual
	Fedotov intensity scale (Fedotov, 1985)	Agential	Momental	Ordinal	Processual
Maritime wind	Beaufort scale (Fry, 1967)	Locational	Momental	Ordinal	Processual
Sea wave	Douglas sea and swell scale (Dunlop, 2008; Owens, 1982)	Locational	Momental	Ordinal	Processual
Tornado	Fujita scale (Fujita, 1971)	Locational	Momental	Numerical	Processual
	Enhanced Fujita scale (Potter, 2007)	Locational	Durational	Ordinal	Consequential
	TORRO scale (Fujita, 1981; Meaden et al., 2007)	Locational	Momental	Numerical	Processual
	Energy scale (Dotzek, 2009)	Locational	Momental	Numerical	Processual
Tropical cyclone	Accumulated cyclone energy index (Bell et al., 2000)	Agential	Durational	Numerical	Processual
	Power dissipation index (Emanuel, 2005)	Agential	Durational	Numerical	Processual
	Hurricane disaster-potential scale (Simpson & Saffir, 1974)	Agential	Momental	Ordinal	Processual
	Hurricane severity index (Hebert et al., 2010)	Agential	Momental	Ordinal	Processual
	Integrated kinetic energy index (Powell & Reinhold, 2007)	Agential	Momental	Numerical	Processual
	Saffir–Simpson hurricane wind scale (National Hurricane Center & Central Pacific Hurricane Center, 2019)	Agential	Momental	Ordinal	Processual
	Typhoon scale (Typhoon Committee, 2018)	Agential	Momental	Ordinal	Processual
	Indian cyclone scale (National Disaster Management Authority, 2008)	Agential	Momental	Ordinal	Processual
	Southwest Indian ocean tropical cyclone scale (World Meteorological Organization, 2016)	Agential	Momental	Ordinal	Processual
	Australian tropical cyclone severity scale (Bureau of Meteorology, 2019)	Agential	Momental	Ordinal	Processual
	Tropical cyclone severity scale (Bloemendaal et al., 2021)	Locational	Durational	Ordinal	Processual

(Continues)

TABLE 1 (Continued)

Hazard	Scale	Spatial dimension	Temporal dimension	Applicational dimension	Indicial dimension
Rainfall	Rainfall intensity (Chow, 1962)	Locational	Momental	Numerical	Processual
Ice storm	Sperry–Piltz ice accumulation index (spia-index.com, 2019)	Locational	Durational	Ordinal	Processual
Hailstorm	Hailstorm intensity scale (The Tornado and Storm Research Organisation, 2021)	Locational	Durational	Ordinal	Processual
Heatwave	Heat index (Bureau of Meteorology, 2010; National Weather Service, 2019a; Steadman, 1979)	Locational	Momental	Numerical	Processual
	Humidex (Government of Canada, 2019)	Locational	Momental	Numerical	Processual
Cold wave	Wind-chill index (Bureau of Meteorology, 2010; Government of Canada, 2017; Met Office, 2019; National Weather Service, 2019b; Osczevski & Bluestein, 2005)	Locational	Momental	Numerical	Processual
Flood	Flood magnitude (England et al., 2019; Jackson, 2013)	Locational	Momental	Numerical	Processual
Drought	Drought magnitude (McKee et al., 1993)	Locational	Durational	Numerical	Processual
	Standard precipitation index (McKee et al., 1993)	Locational	Momental	Numerical	Processual
	Palmer drought severity index (Palmer, 1965)	Locational	Momental	Numerical	Processual
	Crop moisture index (Palmer, 1968)	Locational	Momental	Numerical	Processual
	Surface water supply index (Shafer & Dezman, 1982)	Locational	Momental	Numerical	Processual
	Effective precipitation index (Byun & Wilhite, 1999)	Locational	Momental	Numerical	Processual
	Soil moisture index (Hunt et al., 2009)	Locational	Momental	Numerical	Processual
	Standardized runoff index (Shukla & Wood, 2008)	Locational	Momental	Numerical	Processual
Wildfire	Fireline intensity (Chafer et al., 2004; Keeley, 2009; Rossi et al., 2019)	Locational	Durational	Numerical	Processual
	Radiant heat flux (Rossi et al., 2010, 2019)	Locational	Durational	Numerical	Processual
	Fire severity (Chafer et al., 2004; Keeley, 2009)	Locational	Durational	Ordinal	Consequential
Solar storm	Geomagnetic storm scale (Space Weather Prediction Center, 2011)	Agential	Momental	Ordinal	Processual
	K_p-index (Bartels et al., 1939)	Locational	Momental	Numerical	Processual
	Solar radiation storm scale (Space Weather Prediction Center, 2011)	Agential	Durational	Ordinal	Processual
	Solar flare intensity (Space Weather Prediction Center 2011, 2019)	Agential	Durational	Ordinal	Processual
Explosion	TNT equivalency (Maienschein, 2002)	Agential	Durational	Numerical	Processual
Radiation	Radiation hazard scale (Askin et al., 2017; Centers for Disease Control and Prevention, 2018)	Locational	Momental	Ordinal	Processual
Nuclear accident	Nuclear accident magnitude scale (Smythe, 2011)	Agential	Durational	Numerical	Processual
Infectious disease	Pandemic severity index (Roos & Schnirring, 2007)	Locational	Momental	Ordinal	Consequential
	Influenza transmissibility (Reed et al., 2013)	Locational	Momental	Ordinal	Consequential
	Influenza clinical severity (Reed et al., 2013)	Locational	Momental	Ordinal	Consequential
Multiple hazards	Swiss hazard intensity (Loat, 2010)	Locational	Durational	Ordinal	Processual
	ARMONIA hazard intensity (Kappes et al., 2012)	Locational	Durational	Ordinal	Processual
	Gardoni Scale (Wang & Sebastian, 2021b)	Agential	Durational	Numerical	Processual

Hurricane Center, 2019) is a momental scale that indicates how intense an entire tropical cyclone is at a specific moment in time. However, values of a momental scale for an event can be aggregated to produce one unique value as a proxy durational scale. Instead of using the durational scales listed in Table 1 for tropical cyclones, for example, hurricane researchers tend to use the peak value on the Saffir–Simpson hurricane wind scale to categorize hurricane events (National Hurricane Center & Central Pacific Hurricane Center, 2019).

Combining the types of hazard strength scales along the spatial and temporal dimensions, we can identify four basic

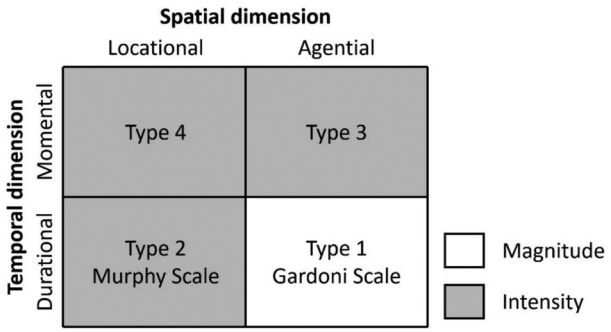

FIGURE 2 Types of hazard strength scales according to categorization along the spatial and temporal dimensions of hazard strength scales. Only the Gardoni Scale (Wang & Sebastian, 2021b) and the proposed Murphy Scale are plotted in this figure

types of hazard strength scales (see Figure 2). The first type is the agential-durational scale; the second is the locational-durational scale; the third is the agential-momental scale; and the fourth is the locational-momental scale. The term *magnitude* is usually used in hazard literature to refer to a Type 1 agential-durational scale, except for few types of hazard events including floods and droughts (England et al., 2019; Jackson, 2013; McKee et al., 1993). In the meantime, the term *intensity* can be used for any of the other three types of hazard strength scales, except for few scales, such as the solar flare intensity (Space Weather Prediction Center, 2011, 2019), that are agential-durational. Accordingly, in this article, we suggest using the term magnitude to refer to a Type 1, or agential-durational, scale and the term intensity for the other types of hazard strength scales.

2.1.3 | Applicational dimension

The applicational dimension indicates whether the values on a hazard strength scale are expressed in real numbers potentially for numerical applications or in ordinal categories for hazard communication in general. If a scale may take on any real number value within its range, we describe it as a *numerical scale*. Values on a numerical scale are usually reported as rounded to a certain decimal point. For example, the moment magnitude (Kanamori, 1977) for an earthquake is a numerical scale. In the meantime, a hazard strength scale displayed in ordinal categories is considered an *ordinal scale*. Most of the ordinal scales, for example, the Beaufort scale (Fry, 1967) for maritime wind hazard events and the hailstorm intensity scale (The Tornado and Storm Research Organisation, 2021) for hailstorms, are qualitatively derived from a set of numerical measures of hazard strengths. Meanwhile, some other ordinal scales, such as the integrated tsunami intensity scale (Lekkas et al., 2013) for tsunami, are partially or entirely based on descriptions of observations.

Practically, a numerical hazard strength scale can be relatively easily transformed into ordinal categories. Without sufficient information on such transformation, however, it may be difficult to convert an ordinal scale back into a numerical one. Regarding a hazard strength scale, a numerical form may be preferred for technical computation for analysis and prediction of vulnerability, resilience, and risk with a high precision. Meanwhile, a hazard strength scale with an ordinal or categorical appearance may be more user-friendly, when the scale is adopted for hazard communication toward different stakeholders, especially the public.

2.1.4 | Indicial dimension

The indicial dimension displays if a hazard strength scale is constructed as a function of indicators of the process of a hazard event or indicators of the negative consequences of the event. We call hazard strength indicators *processual indicators* when they measure the process of the event from its onset to dissipation while approaching and reaching the entities of interest exposed to the event. In the meantime, hazard strength indicators are called *consequential indicators* if they indicate the adverse impact or negative consequences observed during or after the hazard event. Accordingly, we call a hazard strength scale a *processual scale* or *consequential scale* if it is a function of processual indicators or consequential indicators, respectively. For example, the Fujita scale for tornadoes was initially developed as a processual scale based on the gust wind speed of a tornado (Fujita, 1971). However, the in situ processual measurements of gust wind speed of tornadoes are difficult to obtain. Thus, an enhanced Fujita scale was later proposed to use consequential indicators of postevent expert evaluations of damages to estimate the intensity of a tornado (Potter, 2007). Although consequential indicators may be adopted, we would recommend using processual indicators for constructing a hazard strength scale, because consequential indicators are likely to be biased due to factors of exposed value and vulnerability of entities of interest to the hazard event (Doswell et al., 2009).

For some hazard strength scales, a mixture of processual and consequential indicators may be used. For example, the integrated tsunami intensity scale is derived from one processual and five consequential indicators (Lekkas et al., 2013). Some other hazard strength scales may be originally designed to be based on consequential indicators but later developed into processual scales. As an example, the modified Mercalli intensity scale was initially proposed as a consequential scale based on indicators of impact of ground shaking (Wood & Neumann, 1931). Later, during their effort to create ShakeMaps (Wald et al., 2006) for earthquake events, the United States Geological Survey (USGS) developed a quantitative method to derive the modified Mercalli intensity scale with processual indicators such as PGA and peak ground velocity (PGV).

2.2 | Equivalent hazard strength scales

Despite the abundance of singular hazard strength scales, few scholarly efforts have been dedicated to studying and developing hazard strength scales that can be used across hazard types. Recently, Wang and Sebastian proposed an equivalent agential-durational hazard strength scale—the Gardoni Scale (Wang & Sebastian, 2021b). However, the Gardoni Scale is an agential scale for measuring the hazard strength of the spatial and temporal entirety of a hazard event. An agential scale is insufficient for detailed spatial analysis for disaster risk studies because detailed spatial analysis for disaster risk studies requires locational hazard strength metrics for computation. Regarding locational hazard strength scales for multiple hazards, the existing scales such as the Swiss hazard intensity (Loat, 2010) and ARMONIA hazard intensity (Kappes et al., 2012) have their limitations due to two reasons. First, no empirical evidence based on historical data was used to support the development of these existing multi-hazard locational scales. For these multi-hazard locational scales, the categories of event intensities across different hazards were determined subjectively by the modelers. Moreover, these existing multi-hazard locational scales were designed as ordinal scales. Thus, they are not suitable for technical computation with a high precision for analysis of vulnerability, resilience, and risk.

2.3 | Murphy Scale

To overcome the limitations of existing multi-hazard locational hazard strength scales, we propose in this article the Murphy Scale to refer to the Type 2, or locational-durational, hazard strength scale for multiple hazard types, as shown in Figure 2. We further suggest using the term *hazard equivalency* to refer to a new area of research to study and model the equivalent relationships between hazard events and hazard conditions across hazard types within a multi-hazard context. Although a Murphy Scale is a locational scale, it can be converted into an agential Gardoni Scale through aggregation of values on the Murphy Scale across the entire spatial range of a hazard event to derive a unique value associated with the hazard event. The Murphy Scale is also proposed as a numerical scale suitable for multi-hazard hazard mapping and technical computation for analysis of vulnerability, resilience, and risk. However, the Murphy Scale can be easily converted into an ordinal form to appeal to different stakeholders for hazard communication. Ideally, a Murphy Scale is a processual scale corresponding to the equivalent intensity as a function of indicators of the process of a hazard event. When records of processual indicators are difficult to obtain, consequential indicators may also be used to support the development and computation of the Murphy Scale. Since the proposed Murphy Scale is a locational scale along the spatial dimension, different versions of the scale can be developed to correspond to different spatial resolutions.

3 | GENERAL METHODOLOGY

To derive a Murphy Scale, we propose an empirical methodology with a machine learning approach. The equivalent intensity on a Murphy Scale is modeled as a function of locational-durational intensity indicators of a hazard event. Meanwhile, we can calibrate the model parameters by associating the equivalent intensity on a Murphy Scale with historical data on adverse impacts of hazard events. In this way, although drivers of damage due to hazard events may differ with regards to different hazard types, the negative consequences of hazard events provide a common metric to indicate the intensities of hazard events (Hillier & Dixon, 2020; Hillier et al., 2015; Wang & Sebastian, 2021b).

The equivalent intensity on a Murphy Scale is defined as a function of intensity indicators, as

$$EI := q_i\left(II_{i,1},\ II_{i,2}, \cdots, II_{i,m_i}\right), \tag{1}$$

where EI is the equivalent intensity on the Murphy Scale, $q_i(\cdot)$ is the function for computing EI regarding the ith type of hazard, $II_{i,j}$ is the jth intensity indicator of the ith type of hazard, and m_i is the total number of intensity indicators for the ith type of hazard. Table 2 lists examples from the literature of locational processual intensity indicators that can potentially be used for derivation of Murphy Scale. Here, the momental indicators in Table 2 can be converted into durational indicators to facilitate computation of EI on a Murphy Scale.

After reducing biases due to factors of exposed value and hazard vulnerability, we can associate the equivalent intensity on a Murphy Scale with the expectation of a consequence metric indicating the level of adverse impacts of a hazard event. We will discuss how to reduce such biases in Section 5. The formula for the relationship between equivalent intensity and the consequence metric is

$$EI = \hat{\mathrm{E}}\left[g\left(D_1,\ D_2,\ \cdots,\ D_{NCM}\right)\right], \tag{2}$$

where $\hat{\mathrm{E}}[\cdot]$ refers to the point estimate of the expectation, $g(\cdot)$ is the function giving the consequence metric, D_h is the hth measure of the adverse consequences, and NCM is the total number of consequence measures. These consequence measures may include casualties, mental or physical health impact, loss of property and economic wellbeing, infrastructure disruption, loss of livelihood, loss of social capital, and business interruption (Alexander, 2013; Boakye et al., 2019; Lindell & Prater, 2003; Nocera & Gardoni, 2019; Wang et al., 2016). The consequence measures are not consequential intensity indicators. They are only used to produce the consequence metric to calibrate the model of equivalent hazard intensity.

TABLE 2 Examples of potential locational processual intensity indicators for computing the equivalent intensity on a Murphy Scale

Hazard	Intensity indicator
Earthquake	Peak ground acceleration (Open Source Seismic Hazard Analysis, 2010)
	Peak ground velocity (Open Source Seismic Hazard Analysis, 2010)
	Peak ground displacement (Open Source Seismic Hazard Analysis, 2010)
	Spectral acceleration (Open Source Seismic Hazard Analysis, 2010)
Tsunami	Distance inland flooded by tsunami (Ambraseys, 1962)
	Maximum tsunami wave height (Shuto, 1993)
	Mean tsunami wave height (Shuto, 1993)
	Local tsunami wave crest height above ground level at shoreline (Shuto, 1993)
	Tsunami flow depth (Lekkas et al., 2013)
Landslide	Landslide volume (Singh et al., 2019)
	Landslide expected velocity (Singh et al., 2019)
Volcanic activity	Sulfur dioxide concentration (Schmidt et al., 2015)
	Ash cloud mass loading (Corradini et al., 2016)
	Aerosol optical depth at 550 nm (Corradini et al., 2016)
	Effective radius of ash cloud particles (Corradini et al., 2016)
	Concentration of ash mass (Corradini et al., 2016)
	Altitude of ash cloud (Corradini et al., 2016)
	Ash cloud vertical thickness (Corradini et al., 2016)
	Pyroclastic deposit volume (Pallister et al., 2019)
Strong wind	3-second gust wind speed (Lombardo, 2012)
	10-minute average wind speed at 10 m above ground level (Royal Meteorological Society, 2018)
Sea wave	Average wave height (Dunlop, 2008; Owens, 1982)
Tornado	3-second gust wind speed (Potter, 2007; Royal Meteorological Society, 2018)
Tropical cyclone	Sustained wind speed (National Oceanic and Atmospheric Administration, 2020)
	3-second gust wind speed (Royal Meteorological Society, 2018)
	Rainfall (Mudd et al., 2017)
Rainfall	Peak rainfall intensity (Brown, 2016)
Ice storm	Maximum radial ice thickness (spia-index.com, 2019)
	Peak wind velocity (spia-index.com, 2019)
Hailstorm	Maximum hail diameter (The Tornado and Storm Research Organisation, 2021)
	Peak wind velocity (The Tornado and Storm Research Organisation, 2021)
Heat wave	Temperature (Bureau of Meteorology, 2010; National Weather Service, 2019a; Steadman, 1979)
	Relative humidity (Bureau of Meteorology, 2010; National Weather Service, 2019a; Steadman, 1979)
Cold wave	Temperature (Bureau of Meteorology, 2010; Government of Canada, 2017; Lombardo et al., 2014; Met Office, 2019; National Weather Service, 2019b; Osczevski & Bluestein, 2005)
	Wind speed (Bureau of Meteorology 2010; Government of Canada 2017; Lombardo et al., 2014; Met Office 2019; National Weather Service 2019b; Osczevski & Bluestein, 2005)
Flood	Maximum water depth (van de Lindt et al., 2020; Wang & Sebastian, 2021a)
	Water surface elevation (Couasnon et al., 2018)
Drought	Long-term precipitation (Mishra & Singh, 2010)
	Temperature (Mishra & Singh, 2010)
	Weekly moisture conditions (Mishra & Singh, 2010)
	Snowpack (Mishra & Singh, 2010)
	Streamflow (Mishra & Singh, 2010)
	Reservoir storage (Mishra & Singh, 2010)
	Vegetation dynamics (Mishra & Singh, 2010)
	Soil water content (Mishra & Singh, 2010)

(Continues)

TABLE 2 (Continued)

Hazard	Intensity indicator
Wildfire	Heat yield (Chafer et al., 2004)
	Available fuel (Chafer et al., 2004)
	Rate of forwards fire spread (Chafer et al., 2004)
	Time-averaged energy flux (Keeley, 2009)
Solar storm	Maximum magnetic fluctuation (Bartels et al., 1939)
	Peak flux of ions with energy greater than 10 MeV in 5 min (Space Weather Prediction Center, 2011)
Radiation	Radiation dose (Askin et al., 2017; Centers for Disease Control and Prevention, 2018)

Once the consequence metric g is determined, we can apply a supervised machine learning approach to establish a model

$$g = q_i\left(II_{i,1}, II_{i,2}, \cdots, II_{i,m_i}, \theta_i\right) \tag{3}$$

where θ_i is the vector of model parameters for the ith type of hazard. With historical data on adverse impacts and intensity indicators, model of Equation (3) can be calibrated, and the result is

$$EI = \hat{\mathrm{E}}[g(D_1, D_2, \cdots, D_{NCM})] = \hat{q}_i(II_{i,1}, II_{i,2}, \cdots, II_{i,m_i}, \hat{\theta}_i), \tag{4}$$

where $\hat{q}_i(\cdot)$ and $\hat{\theta}_i$ are, respectively, the prediction of the calibrated model and the point estimate of model parameters.

4 | EXAMPLE APPLICATION

To illustrate the proposed methodology, we applied a Bayesian binomial regression approach (Wang et al., 2020) using observed historical data on adverse impacts of earthquakes and tropical cyclones to develop a prototype version of Murphy Scale for earthquake and tropical cyclone. The derived equivalent intensity on the Murphy Scale can be interpreted as the expected probability of experiencing damage due to a hazard event at a location. The demonstration of the prototype example was achieved by using programing language Python (Python Software Foundation, 2020).

4.1 | Data

For the example application, we compiled two datasets containing data points of damages due to earthquakes and tropical cyclones, respectively, that occurred during a period from 2013 to 2017 worldwide. We only kept data points from 2013 to reduce the potential bias in data because of a different protocol adopted by the Earthquake Impact Database to record impacts of events before 2013 (see, e.g., Wang et al., 2020). For this study, the final earthquake and tropical cyclone datasets contain 1063 and 575 data points, respectively (Guha-Sapir et al., 2020; National Centers for Environmental Information, 2018; National Oceanic and Atmospheric Administration, 2020; Wang et al., 2020). The spatial resolution of the two datasets is at the country level. Therefore, each data point in the datasets refers to a country that experienced an earthquake or tropical cyclone event. The earthquake dataset was based on 937 earthquakes with a moment magnitude (Kanamori, 1977) equal to or larger than 5.0 (Guha-Sapir et al., 2020; National Centers for Environmental Information, 2018; Wang et al., 2020). Meanwhile, the tropical cyclone dataset was compiled from data on 320 tropical cyclones with their eyes having passed within 50 km from a populated continental region or island (Guha-Sapir et al., 2020; National Oceanic and Atmospheric Administration, 2020). For each hazard, there were more data points than events because each event may have affected more than one countries.

Considered damages include fatalities, injuries, and economic losses caused by the hazard events and their associated secondary hazard conditions. The secondary hazard conditions for earthquake include rockfall, nonstructural damage, and structural failure, except tsunami. Wind gust, water surge, and inland flooding contributed to the damages associated with tropical cyclone events. For each considered hazard event, only one intensity indicator was adopted due to limited availability of data. Damage data were collected from online sources including the International Disaster Database EM-DAT (Guha-Sapir et al., 2020) and the National Centers for Environmental Information (NCEI) (National Centers for Environmental Information, 2018). Economic losses were converted to 2019 United States Dollars (USD) using the consumer price index. Nonzero economic losses were recorded only for events exceeding an economic loss of 1 million USD. The intensity indicator for earthquake is the natural logarithm of on-land PGA in meters per squared second (m/s^2) within a country. The records of PGA were computed based on the USGS ShakeMaps (US Geological Survey, 2018; Wald et al., 2006) and shapefiles of country boundaries (Global Administrative Areas, 2018; Wang et al., 2020). For tropical cyclone, the intensity indicator is the natural logarithm of PSWS in kilometers per hour (km/h) within or close to a country. The purpose of the logarithmic transformation of the PGA and PSWS was to convert the range of values of these indicators from $(0, \infty)$ to $(-\infty, \infty)$.

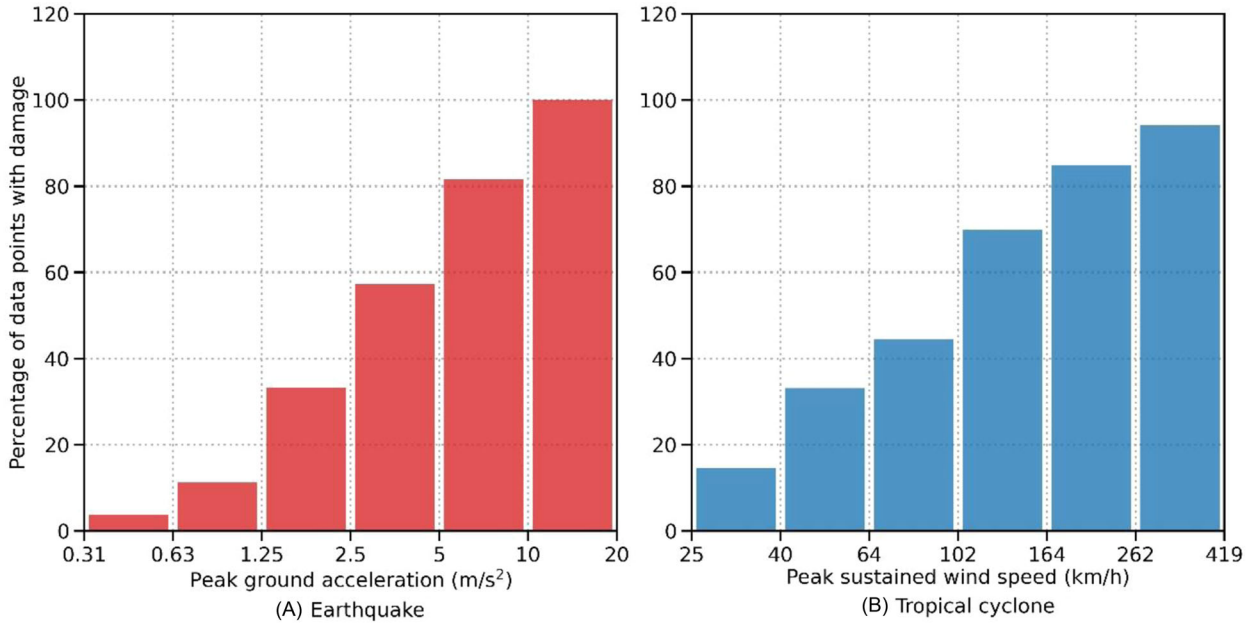

FIGURE 3 Distributions of percentage of data points with observed consequence metric equal to one with respect to (A) peak ground acceleration for earthquake and (B) peak sustained wind speed for tropical cyclone

4.2 | Method

4.2.1 | Consequence metric

To fit the binomial regression method adopted in this study, the observed consequence metric was designed to be binary to have a value of either zero or one. The observed consequence metric equals one when there were nonzero fatalities, nonzero injuries, or nonzero economic losses associated with a hazard event. The observed consequence metric equals zero when the hazard event was recorded with zero fatalities, zero injuries, and zero economic losses. The expectation of consequence metric is, accordingly, an expected probability that the consequence metric equals one. The formula for the consequence metric is

$$g = 1 - \mathbf{1}_{\{0\}}(D_1) \cdot \mathbf{1}_{\{0\}}(D_2) \cdot \mathbf{1}_{\{0\}}(D_3), \quad (5)$$

where $\mathbf{1}_{\{0\}}(D_h)$ is the indicator function that equals one if $D_h = 0$ and zero otherwise, D_1 is the number of fatalities, D_2 is the number of injuries, D_3 is the economic loss, and g is the observed consequence metric. Among all earthquake data points, there are 808 data points where the observed consequence metric is equal to zero and 255 equal to one. For tropical cyclone, there are 292 and 283 data points with zero and nonzero observed consequence metrics, respectively. Figure 3(A and B) show the distributions of percentage of data points with observed consequence metric being one with respect to PGA for earthquakes and PSWS for tropical cyclones. In both cases, the percentage monotonically increases with the increase of the value of intensity indicator. Such a positive correlation can be captured with a binomial regression model.

4.2.2 | Binomial regression model

Binomial regression is a supervised machine learning approach that can be used to predict the expected probability of a data point associated with one of two possible values. It is suitable for the purpose of the example application for deriving the equivalent intensity on the Murphy Scale for hazard events herein. The probability mass function (PMF) for a binomial regression model can be written as

$$f_{\mathrm{A}}(g|\alpha) = \alpha^{\mathbf{1}_{\{1\}}(g)}(1-\alpha)^{\mathbf{1}_{\{0\}}(g)}, \quad (6)$$

where $\alpha \in (0, 1)$ is the mean function regarding the intensity indicator and model parameters.

A common approach to establish a binomial regression model is to adopt the cumulative distribution function (CDF) of a standard logistic random variable as the mean function (Cox, 1958; Wang et al., 2020). Such a regression approach is also called a logistic regression. Its mean function is

$$\boldsymbol{\alpha} = \frac{\exp(\beta + \gamma \boldsymbol{II})}{1 + \exp(\beta + \gamma \boldsymbol{II})}, \quad (7)$$

where $\boldsymbol{\alpha}$ is the vector of the expected values of consequence metric, $\boldsymbol{II}$ is the vector of observations of intensity indicator, β is the coefficient of intercept, γ is the coefficient of $\boldsymbol{II}$. Both β and γ are model parameters as in θ_i in Equation (3).

Since the numbers of observed zeroes and ones of the consequence metric are not equal, a rare-event subsampling approach was used (King & Zeng, 2001). Because there are more zero data points than nonzero data points for both earthquakes and tropical cyclones, for each hazard, we randomly selected from the entire pool of zero data points the same number of zero data points as the nonzero data points. The selected zero data points were then used along with all nonzero data points for model calibration.

4.2.3 | Bayesian approach

To allow the parameters to be updated with new data that will become available in the future, the authors adopted a Bayesian approach to estimate the model parameters (Andreini et al., 2016; Gardoni et al., 2002, 2007; Wang et al., 2020). The general Bayesian updating rule is (Box & Tiao, 1992)

$$f''(\boldsymbol{\theta}) = \mathrm{k}\, L(\boldsymbol{\theta})\, f'(\boldsymbol{\theta}), \tag{8}$$

where $f''(\boldsymbol{\theta})$ is the posterior probability density function (PDF) of parameters $\boldsymbol{\theta}$ given observations, $f'(\boldsymbol{\theta})$ is the prior PDF of $\boldsymbol{\theta}$, $L(\boldsymbol{\theta})$ is the likelihood function of $\boldsymbol{\theta}$, and

$$\mathrm{k} = \left[\int L(\boldsymbol{\theta})\, f'(\boldsymbol{\theta})\, \mathrm{d}\boldsymbol{\theta}\right]^{-1} \tag{9}$$

is a normalizing constant. Because no prior knowledge about model parameters was available at this stage, the prior PDF of model parameters can be set as a constant.

Given the constant prior, the posterior PDF of the binomial model with the standard logistic mean function is proportional to its likelihood function

$$L(\boldsymbol{\theta}) = \prod_{w=1}^{n} \frac{\exp\left(\boldsymbol{X\theta}\, g_w\right)}{1 + \exp\left(\boldsymbol{X\theta}\right)}. \tag{10}$$

Let $\boldsymbol{\theta} = (\beta, \gamma)^{\mathrm{T}}$, and $\boldsymbol{X}$ be the data matrix including the intercept and $\boldsymbol{II}$. Accordingly, the posterior PDF of the model parameters is

$$f''(\boldsymbol{\theta}) = \mathrm{k} \prod_{w=1}^{n} \frac{\exp\left(\boldsymbol{X\theta}\, g_w\right)}{1 + \exp\left(\boldsymbol{X\theta}\right)}, \tag{11}$$

where g_w is the value of the observed consequence metric of the wth data point and n is the total number of data points for model calibration.

4.2.4 | Importance sampling

To generate the posterior statistics of model parameters, we implemented an importance sampling method by computing the integrals of the general form (Andreini et al., 2016; Gardoni et al., 2002, 2007; Wang et al., 2020)

$$I = \int B(\boldsymbol{\theta})\, d\boldsymbol{\theta}, \tag{12}$$

where

$$B(\boldsymbol{\theta}) = u(\boldsymbol{\theta})\, L(\boldsymbol{\theta})\, f'(\boldsymbol{\theta}), \tag{13}$$

is the Bayesian integrand. When $u(\boldsymbol{\theta}) = 1$, the normalizing constant k in Equation (9) can be computed as the inverse of the integral. If $u(\boldsymbol{\theta}) = \mathrm{k}\boldsymbol{\theta}$, the integral equals to the posterior mean vector $\tilde{\boldsymbol{\theta}}$ of model parameters. When $u(\boldsymbol{\theta}) = \mathrm{k}\boldsymbol{\theta}\boldsymbol{\theta}^{\mathrm{T}}$, the integral, $I = \hat{\mathrm{E}}(\boldsymbol{\theta}\boldsymbol{\theta}^{\mathrm{T}})$, can be used to derive the covariance matrix

$$\hat{\boldsymbol{\Sigma}}_{\boldsymbol{\Theta}} = \hat{\mathrm{E}}\left(\boldsymbol{\theta}\boldsymbol{\theta}^{\mathrm{T}}\right) - \tilde{\boldsymbol{\theta}}\tilde{\boldsymbol{\theta}}^{\mathrm{T}}. \tag{14}$$

With an importance sampling density $S(\boldsymbol{\theta})$, the integral can be written as

$$I = \int \frac{B(\boldsymbol{\theta})}{S(\boldsymbol{\theta})} S(\boldsymbol{\theta})\, d\boldsymbol{\theta} \tag{15}$$

and the sample mean of the integral is

$$\hat{\mathrm{E}}(I) = \frac{1}{N} \sum_{z=1}^{N} \frac{\mathrm{B}\left(\boldsymbol{\theta}_z\right)}{\mathrm{S}\left(\boldsymbol{\theta}_z\right)}, \tag{16}$$

where N is the number of random samples of $\boldsymbol{\theta}$ and $\boldsymbol{\theta}_z$ is the zth simulation of $\boldsymbol{\theta}$. The sample size N is determined by a metric denoted as M_{IS} based on the coefficient of variation of $\hat{\mathrm{E}}(\boldsymbol{\theta}/\mathrm{k})$, as

$$M_{\mathrm{IS}} = \max \left| \frac{\sqrt{\sum_{z=1}^{N} \left[\theta_z L(\theta_z)\, f'(\theta_z) \,/\, S(\theta_z)\right]^2 - \frac{1}{\mathrm{N}}\left\{\sum_{z=1}^{N} \left[\theta_z L(\theta_z)\, f'(\theta_z) \,/\, S(\theta_z)\right]\right\}^2}}{\sum_{z=1}^{N} \left[\theta_z L(\theta_z)\, f'(\theta_z) \,/\, \mathrm{S}(\theta_z)\right]} \right|, \tag{17}$$

where $|\cdot|$ refers to the vector of absolute values. To keep M_{IS} as small as around 10^{-4}, we set $N = 10^4$.

4.3 | Results

Using the proposed modeling and calibration methods, we reached the statistics of parameters of the logistic binomial regression models for earthquake and tropical cyclone. As listed in Table 3, the βs and γs correspond to the parameters in Equation (7). All estimates of parameters have a small p-value, indicating high statistical significance. With the estimated model parameters, we can establish the relationships between the equivalent intensity on the derived Murphy Scale and intensity indicators such as PGA for earthquake and PSWS for tropical cyclone, as shown in Table 4. Such

TABLE 3 Statistics of parameters of binomial models for earthquake and tropical cyclone

Statistic		Earthquake	Tropical cyclone
β	Estimate	−0.6999	−8.4389
	Standard error	0.1203	0.8545
	p-Value	1.0518×10^{-8}	2.5213×10^{-21}
γ	Estimate	1.8035	1.9105
	Standard error	0.1790	0.1932
	p-Value	6.8942×10^{-22}	2.2261×10^{-21}
Correlation coefficient between β and γ		−0.5186	−0.9938

TABLE 4 Equivalent intensities on the derived Murphy Scale and their corresponding peak ground accelerations of earthquakes and peak sustained wind speeds of tropical cyclones

Equivalent intensity on the Murphy Scale	Peak ground acceleration (m/s^2)	Peak sustained wind speed (km/h)
0.1	0.4359	26.2345
0.2	0.6835	40.1066
0.3	0.9215	53.1792
0.4	1.1774	67.0163
0.5	1.4742	82.8613
0.6	1.8459	102.4525
0.7	2.3583	129.1104
0.8	3.1798	171.1934
0.9	4.9851	261.7156

relationships are also visualized in Figure 4(B) as the solid curve. In addition, Figures 4(A and C) display the empirical distributions of data points with zero and nonzero damage, respectively, with respect to intensity indicators. With these computed relationships regarding the proposed Murphy Scale, we can comparatively analyze locational-durational hazard strengths between earthquakes and tropical cyclones. From Table 4 and Figure 4, we can see that an equivalent intensity of 0.4 on the Murphy Scale with a spatial resolution at the country level is equivalent to an earthquake PGA of about 1.2 m/s^2 and a tropical cyclone PSWS of 67 km/h, slightly above the boundary between the PSWSs of a tropical depression and a tropical storm. On the other hand, a 0.9 equivalent intensity on the Murphy Scale corresponds to a 5 m/s^2 PGA and a 262 km/h PSWS, a peak wind speed of a Category 5 hurricane on the Saffir–Simpson hurricane wind scale (National Hurricane Center & Central Pacific Hurricane Center, 2019).

Because we adopted a random selection process for rare-event subsampling (King & Zeng, 2001) for binomial regression and a Monte Carlo simulation (Metropolis & Ulam, 1949) during model calibration with the importance sampling approach (Wang et al., 2020), different runs of the Python codes used for this study would yield slightly different sets of estimates of model parameters. To evaluate the extent to which such uncertainties associated with these parametric estimations would affect the performance of proposed models, we conducted 1000 iterations of subsampling twofold cross-validations for both earthquake and tropical cyclone data points. As shown by the 95% confidence intervals of receiver operating characteristic curves (Fawcett, 2006) in Figure 5, the effect of the uncertainties on the overall model performance is small.

5 | DISCUSSION

After the delineation of definition of Murphy Scale and demonstration of its computational methodology, in this section, we outline and discuss the potential applications of Murphy Scale, its relationships with singular hazard strength metrics, future research to improve its formulation, and the data requirements for its computation.

5.1 | Potential applications

The proposed Murphy Scale can be widely applied for technical computation for analysis of hazard, resilience, and risk across hazard types. First, the equivalent intensity on a Murphy Scale can be used to represent intensity indicators such as the ones on the horizontal axis in Figure 1 for quantification of vulnerability and resilience with an empirical predictive modeling approach. Then, instead of using one event intensity metric for one hazard type only, hazard modelers can create hazard maps based on the equivalent intensity on a Murphy Scale to display the geographical distribution of exceedance probability of hazard event intensity at locations. The adoption of the Murphy Scale would enable the integration of information on hazard event intensity exceedance associated with different hazards into one multi-hazard hazard map. Using a multi-hazard vulnerability and resilience analysis and a multi-hazard hazard map with the implementation of a Murphy Scale, we can significantly simplify calculations of expected future losses due to hazards while maintaining a high accuracy of these calculations to facilitate decision making for hazard planning and management. In this manner, the adoption of a Murphy Scale will benefit many risk-related industries such as agriculture, banking, civil infrastructure, and homeland security (Buck &

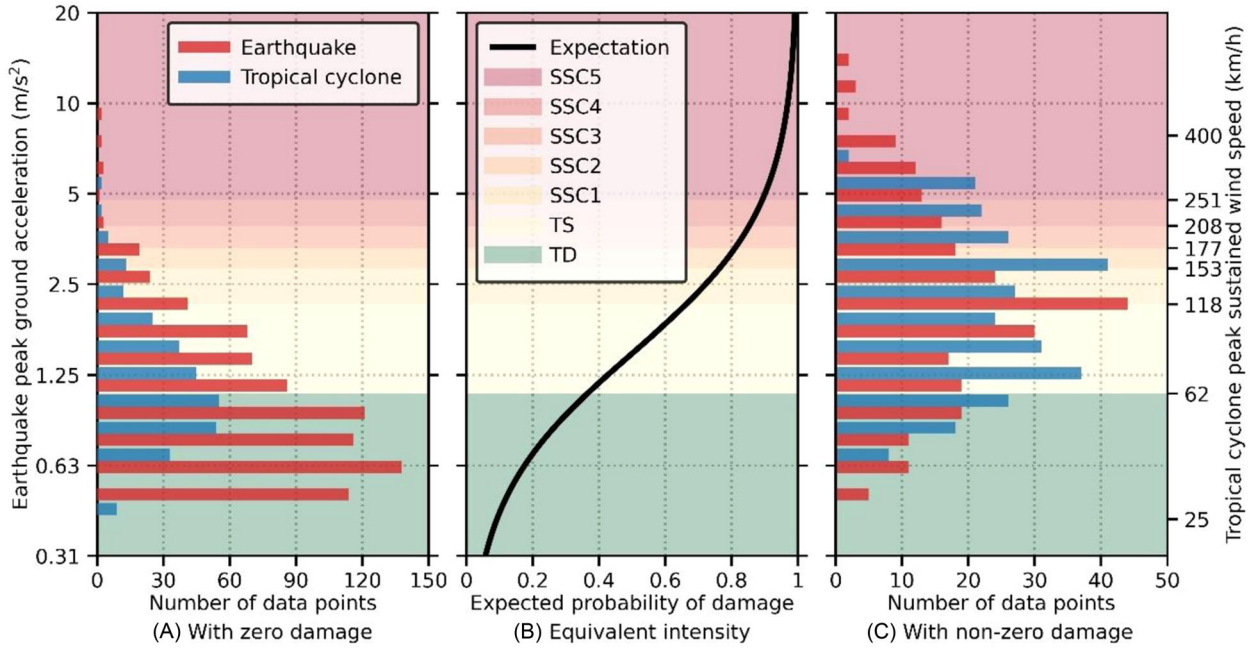

FIGURE 4 Relationships between equivalent intensity on the derived Murphy Scale and intensity indicators of earthquakes and tropical cyclones. (A) The distribution of data points with zero damage with respect to intensity indicators. (B) The expectation of probability of damage as the equivalent intensity on the Murphy Scale as a function of earthquake peak ground acceleration or a function of tropical cyclone peak sustained wind speed. SSC5, SSC4, SSC3, SSC2, and SSC1 refer to Saffir–Simpson hurricane wind scale (National Hurricane Center & Central Pacific Hurricane Center, 2019) Categories 5, 4, 3, 2, and 1, respectively; TS refers to tropical storm; and TD is short for tropical depression. (C) The distribution of data points with non-zero damage with respect to intensity indicators

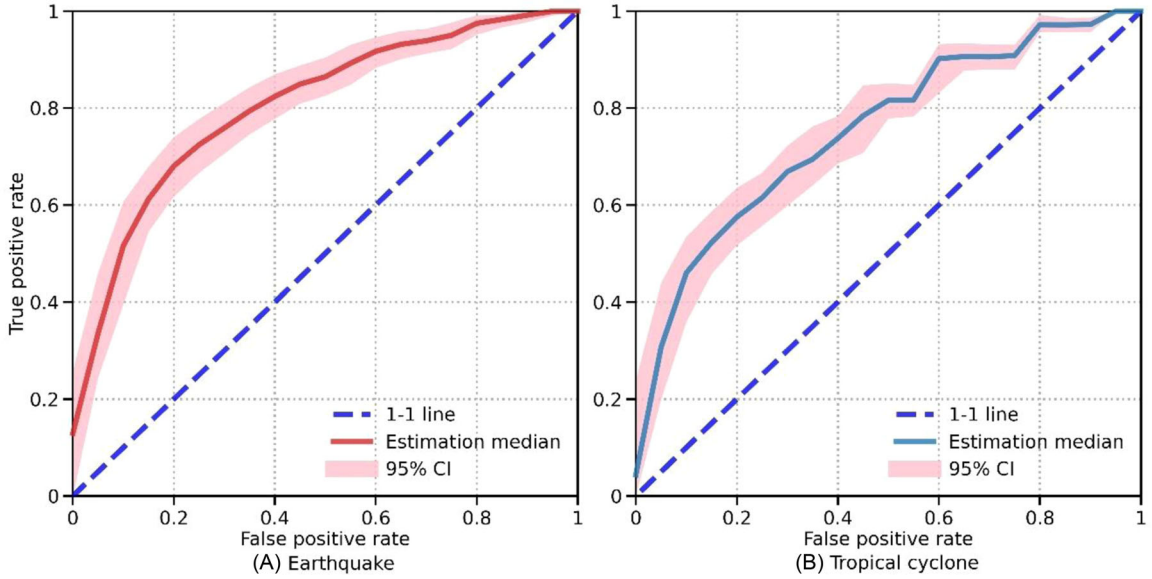

FIGURE 5 Receiver operating characteristic curves (Fawcett, 2006) of logistic binomial regression models for (A) earthquake and (B) tropical cyclone, based on 1000 iterations of subsampling twofold cross-validations

Summers, 2020; Dabbeek & Silva, 2020; Dilley et al., 2005; Federal Emergency Management Agency, 2020; Kameshwar & Padgett, 2014; Koks et al., 2019; Xu et al., 2019).

Whether with its values further transformed into ordinal categories or in the original numerical form, the proposed Murphy Scale can also be used to facilitate hazard communication. Traditional practices of hazard communication tend to use singular hazard strength metrics for events of their corresponding hazard types. However, these metrics usually adopt incompatible categories and ranges to refer to the expected

severities of hazard events of different hazard types, especially for locational purposes. For example, an earthquake locational-durational intensity is measured between I and X on the modified Mercalli intensity scale (Wald et al., 2006; Wood & Neumann, 1931); a tornado locational-durational intensity is recorded from 0 to 5 on the enhanced Fujita scale (Potter, 2007); and a tropical cyclone locational-durational intensity may be associated with a value between 0 and 6 on the tropical cyclone severity scale (Bloemendaal et al., 2021). Albeit described with different units and categories, these scales are usually used to evaluate the same type of information on the expectation of loss given average exposed value and vulnerability at a location. The proposed Murphy Scale can be used to provide mathematical mappings between these intensity scales for singular hazards. Moreover, when simplicity is preferred especially in hazard communication, professionals can adopt one single metric based on a fully developed Murphy Scale to sufficiently convey, to different stakeholders, information on locational-durational intensities of hazard events across hazard types, instead of having to resort to a myriad of intensity metrics for their corresponding hazards.

5.2 | Relationships with singular hazard strength scales

Despite its potential applications, the Murphy Scale is not intended to completely replace the existing singular hazard strength scales. First, there is only one value on a Murphy Scale corresponding to the intensity of one hazard event at one location. Such a value does not reveal the rich information that is usually conveyed by studying and modeling singular hazard strength scales. For a comprehensive understanding of phenomena underlying the computation of the equivalent intensity on a Murphy Scale, knowledge regarding singular hazard strength scales will always play an important role and the derivation of singular hazard strength scales provides the foundation for formulation and computation of a Murphy Scale. In addition, for some hazard events such as tornadoes (Potter, 2007), for which processual intensity indicators are difficult to obtain, the developed singular hazard strength scales may be used to estimate the intensity indicators or directly as one intensity indicator for computation of equivalent intensity on a Murphy Scale.

5.3 | Formulation for computation

The proposed Murphy Scale refers to the Type 2 equivalent hazard strength scale, as shown in Figure 2. Its formulation is not unique. There are unlimited numbers of mathematical models that can be used to formulate a Murphy Scale. In this article, for example, we only suggested one approach—the Bayesian logistic binomial regression (Wang et al., 2020)—to compute the equivalent intensity on a Murphy Scale. As a result, the derived values of equivalent intensity are between zero and one where each of the values corresponds to the expected probability that an entity of interest at a location will experience damage in terms of casualty or economic loss given an average exposed value and vulnerability. Other formulations of Murphy Scale may also be developed, resulting in different ranges and meanings of the values of equivalent intensity. The manifestation of the meanings of a Murphy Scale depends on the design of the consequence metric described by Equation (2). The proposal and improvement of such designs of the consequence metric require more comprehensive interdisciplinary research in the future.

In addition to the consequence metric of Murphy Scale, intensity indicators of Murphy Scale may also need to be systematically studied. As shown in Table 2, for example, intensity indicators for earthquake that may be considered for computation of Murphy Scale also include PGV, peak ground displacement, and spectral accelerations at different frequencies (Open Source Seismic Hazard Analysis, 2010). In this article, we only used the natural logarithm of PGA as the sole intensity indicator. Similarly, for tropical cyclone, we only adopted the natural logarithm of PSWS as the sole intensity indicator. However, the gust wind speed and rainfall measures are also important in determining whether there are consequences from an event and, thus, may also be included as the intensity indicators for computation of Murphy Scale (see, e.g., Mudd et al., 2017; Royal Meteorological Society, 2018). Whether the inclusion of other intensity indicators may improve the computation of Murphy Scale is yet to be explored. Along this line, future work needs to experiment with data on intensity indicators and negative consequences of hazard events to seek the most appropriate combination of intensity indicators and functions of these intensity indicators regarding the considered consequence metrics.

5.4 | Data requirements

To support the proposed data-driven machine learning methodology for computation of Murphy Scale, large volumes of data on hazard consequences and intensity indicators are needed. However, currently available historical records of hazard events are usually poor in quality in terms of coarse spatial and temporal resolutions as well as potential biases. More scholarly efforts are, therefore, needed to reconstruct historical records of hazard events with high spatial and temporal resolutions (e.g., Earle et al., 2009; Forebes et al., 2010; Mayo & Lin, 2019; Paprotny et al., 2018). In the meantime, since hazard consequences can be influenced by factors of exposed value and local vulnerability, historical records of hazard consequences may lead to bias in the estimation of equivalent intensity on a Murphy Scale. To reduce this bias, a large sample size is needed. In addition, samples of these hazard event records need to be distributed as widely as possible both spatially and temporally for each hazard type.

Simultaneously, due to spatial and temporal changes in vulnerability, there is also a need to ensure that records of events occurred in a same geographical region and temporal

period to generate a complete picture of distribution of equivalent intensities of hazard events on a Murphy Scale. Given identical exposed values, for example, suppose that data on earthquake and tropical cyclone records are collected from communities with high and low vulnerability, respectively. In such a case, the derived equivalent intensities on the Murphy Scale for earthquake and for tropical cyclone will, respectively, overestimate and underestimate the true hazard intensity given average vulnerability. On another occasion, suppose vulnerability decreases throughout time for communities in a same region. When earthquake and tropical cyclone records are based on the same communities but pertain to events that occurred in the 20th and 21st centuries, respectively, the equivalent intensity on the Murphy Scale for earthquake will tend to indicate higher intensity than the equivalent intensity on the Murphy Scale for tropical cyclone. Once the quantitative models for Murphy Scale are established, this type of bias of estimate from the true intensity is difficult to detect without the knowledge regarding how the Murphy Scale has been developed and data for computation have been collected in the first place.

In addition, to ensure that a developed Murphy Scale can be used for multiple hazards in a reliable manner, the spatial resolution of data points for different hazards needs to be kept identical. The reason for this is that consequences and intensity indicators at different spatial resolutions may convey inconsistent information on the meanings of Murphy Scale. In this paper, for example, the spatial resolution of data on consequences and intensity indicators is at the country level. The derived equivalent intensity on Murphy Scale indicates the expected probability that a country experiences damage due to a hazard event. This probability may be much higher than the one for a county, a village, or a grid cell of one arc minute, because data on consequences of entities with locations at a lower spatial resolution are aggregated from the entities with locations at a higher spatial resolution. Therefore, to develop a model for the Murphy Scale consistent with the one presented in this article for another hazard, say, riverine flood, the spatial resolution of data on consequences and intensity indicators of riverine floods also needs to be at the country level. When data of finer spatial resolution becomes available, future work also needs to explore and compare the effects of using different spatial resolutions for computation of Murphy Scale.

6 | CONCLUSION

To enable comparative evaluation of locational hazard strengths of hazard events for cross-hazard analysis of vulnerability, resilience, and risk, we propose in this article the Murphy Scale to measure the equivalent intensities of hazard events experienced by local entities of interest. To delineate the conceptual domain of the proposed Murphy Scale, we reviewed existing hazard strength scales and created a typology based on four dimensions, that is, spatial, temporal, applicational, and indicial dimensions. This study contributes to the science of disaster risk, as it presents a typology of existing hazard strength scales and a novel empirical method to compute equivalent hazard intensities across hazard types. In addition, it initiates the scientific inquiries for general development of knowledge in an emerging area of research, called hazard equivalency, for comparative analyses of hazards across hazard types.

Future work should focus on expanding current studies in hazard equivalency by upgrading the typological system for hazard strength scales and exploring other types of equivalent hazard strength scales. Additional work is also needed to improve studies in intensity indicators and consequence metrics for establishing models to compute equivalent hazard strengths on these scales. Moreover, to support data-driven machine learning-based approaches to quantifying equivalent hazard event intensities, more high-quality data on intensity indicators and adverse impacts of hazard events need to be collected. Accordingly, a variety of machine learning and other computational methods may be attempted to optimize the formulation and computation of equivalent hazard strength scales such as the proposed Murphy Scale.

ACKNOWLEDGMENTS

The authors thank Chapman University for financial support for open access publication. We also thank the anonymous reviewers for constructive comments that prompted improvement of the article. Yi Victor Wang (YVW) thanks Professor Colleen Murphy and Professor Paolo Gardoni at the University of Illinois at Urbana-Champaign for inspiring discussions and suggestions that sparked the idea of the study. YVW also acknowledges the nurturing atmosphere at Jackson State University in Jackson, Mississippi, where the study was initiated.

ORCID

Yi Victor Wang https://orcid.org/0000-0003-2228-7009
Antonia Sebastian https://orcid.org/0000-0002-4309-2561

REFERENCES

Abe, K. (1979). Size of great earthquakes of 1837-1974 inferred from tsunami data. *Journal of Geophysical Research*, *84*(B4), 1561–1568.

Ahmed, B., & Kelman, I. (2018). Measuring community vulnerability to environmental hazards: A method for combining quantitative and qualitative data. *Natural Hazards Review*, *19*(3), 04018008.

Alexander, D. E. (2013). Impact, definition of. In K. B. Penuel, M. Statler, & R. Hagen (Eds.), *Encyclopedia of crisis management* (pp. 488–490). SAGE Publications.

Alexander, D. E. (2018). A magnitude scale for cascading disasters. *International Journal of Disaster Risk Reduction*, *30*, 180–185.

Ambraseys, N. N. (1962). Data for the investigation of the seismic sea-waves in the Eastern Mediterranean. *Bulletin of the Seismological Society of America*, *52*(4), 895–913.

Andreini, M., Gardoni, P., Pagliara, S., & Sassu, M. (2016). Probabilistic models for erosion parameters and reliability analysis of earth dams and levees. *ASCE–ASME Journal of Risk and Uncertainty in Engineering Systems, Part A: Civil Engineering*, *2*(4), 04016006.

Arbanas, S. M., & Arbanas, Ž. (2015). Landslides: A guide to researching landslide phenomena and processes. In N. Gaurina–Medjimurec (Ed.), *Handbook of research on advancements in environmental engineering* (pp. 474–510). IGI Global.

Askin, A., Buddemeier, B., Alai, M., & Yu, K. (2017). *Centers for Disease Control and Prevention (CDC) radiation hazard scale data product review feedback report*. Lawrence Livermore National Laboratory. https://e-reports-ext.llnl.gov/pdf/892276.pdf

Bakkensen, L. A., Fox-Lent, C., Read, L. K., & Linkov, I. (2016). Validating resilience and vulnerability indices in the context of natural disasters. *Risk Analysis*, *37*(5), 982–1004.

Bartels, J., Heck, N. H., & Johnston, H. F. (1939). The three-hour-range index measuring geomagnetic activity. *Terrestrial Magnetism and Atmospheric Electricity*, *44*(4), 411–454.

Bass, B., Torres, J. M., Irza, J. N., Proft, J., Sebastian, A., Dawson, C., & Bedient, P. (2018). Surge dynamics across a complex bay coastline, Galveston Bay, TX. *Coastal Engineering*, *138*, 165–183.

Bell, G. D., Halpert, M. S., Schnell, R. C., Higgins, R. W., Lawrimore, J., Kousky, V. E., Tinker, R., Thiaw, W., Chelliah, M., & Artusa, A. (2000). Climate assessment for 1999. *Bulletin of the American Meteorological Society*, *81*(6), S1–S50.

Birkmann, J. (2013). *Measuring vulnerability to natural hazards: Towards disaster resilient societies* (2nd ed.). United Nations University Press.

Bloemendaal, N., de Moel, H., Mol, J. M., Bosma, P. R. M., Polen, A. N., & Collins, J. M. (2021). Adequately reflecting the severity of tropical cyclones using the new Tropical Cyclone Severity Scale. *Environmental Research Letters*, *16*(1), 014048.

Blong, R. (2003). A review of damage intensity scales. *Natural Hazards*, *29*(1), 57–76.

Boakye, J., Gardoni, P., & Murphy, C. (2019). Using opportunities in big data analytics to more accurately predict societal consequences of natural disasters. *Civil Engineering and Environmental Systems*, *36*(1), 100–114.

Bodas, M., Kirsch, T. D., & Peleg, K. (2020). Top hazards approach – Rethinking the appropriateness of the All-Hazards approach in disaster risk management. *International Journal of Disaster Risk Reduction*, *47*, 101559.

Box, G. E. P., & Tiao, G. C. (1992). *Bayesian inference in statistical analysis*. John Wiley & Sons.

Brown, Jr T. H. (2016). Hydraulics. In D. J. Findley, B. J. Schroeder, C. M. Cunningham, & T. H. Brown, Jr (Eds.), *Highway engineering: Planning, design, and operations* (pp. 641–695). Elsevier.

Buck, K. D., & Summers, J. K. (2020). Application of a multi-risk risk assessment for local planning. *Geomatics, Natural Hazards and Risk*, *11*(1), 2058–2078.

Bureau of Meteorology. (2010). *Thermal comfort observations*. Bureau of Meteorology. http://www.bom.gov.au/info/thermal_stress

Bureau of Meteorology. (2019). *What is a tropical cyclone?* Bureau of Meteorology. http://www.bom.gov.au/cyclone/tropical-cyclone-knowledge-centre/understanding/tc-info/

Byun, H. – R., & Wilhite, D. A. (1999). Objective quantification of drought severity and duration. *Journal of Climate*, *12*(9), 2747–2756.

Centers for Disease Control and Prevention. (2018). *Radiation hazard scale: A tool for communication in nuclear and radiological emergencies*. Centers for Disease Control and Prevention. https://www.cdc.gov/nceh/radiation/emergencies/radiationhazardscale.htm

Chafer, C. J., Noonan, M., & Macnaught, E. (2004). The post-fire measurement of fire severity and intensity in the Christmas 2001 Sydney wildfires. *International Journal of Wildland Fire*, *13*(2), 227–240.

Chow, V. T. (1962). *Hydrologic determination of waterway areas for the design of drainage structures in small drainage basins*. University of Illinois at Urbana–Champaign. www.ideals.illinois.edu/bitstream/handle/2142/4137/engineeringexperv00000i00462.pdf

Corradini, S., Montopoli, M., Guerrieri, L., Ricci, M., Scollo, S., Merucci, L., Marzano, F. S., Pugnaghi, S., Prestifilippo, M., Ventress, L. J., Grainger, R. G., Carboni, E., Vulpiani, G., & Coltelli, M. (2016). A multi-sensor approach for volcanic ash cloud retrieval and eruption characterization: The 23 November 2013 Etna lava fountain. *Remote Sensing*, *8*(1), 58.

Couasnon, A., Sebastian, A., & Morales-Nápoles, O. (2018). A copula-based Bayesian network for modeling compound flood hazard from riverine and coastal interactions at the catchment scale: An application to the Houston Ship Channel, Texas. *Water*, *10*(9), 1190.

Cox, D. R. (1958). The regression analysis of binary sequences. *Journal of the Royal Statistical Society. Series B (Methodological)*, *20*(2), 215–242.

Cutter, S. L. (1996). Vulnerability to environmental hazards. *Progress in Human Geography*, *20*(4), 529–539.

Cutter, S. L., Mitchell, J. T., & Scott, M. S. (2000). Revealing the vulnerability of people and places: A case study of Georgetown county, South Carolina. *Annals of the American Association of Geographers*, *90*(4), 713–737.

Dabbeek, J., & Silva, V. (2020). Modeling the residential building stock in the Middle East for multi-hazard risk assessment. *Natural Hazards*, *100*, 781–810.

Dilley, M., Chen, R. S., Deichmann, U., Lerner-Lam, A. L., Arnold, M., Agwe, J., Buys, P., Kjekstad, O., Lyon, B., & Yetman, G. (2005). *Natural disaster hotspots: A global risk analysis*. The World Bank. https://elibrary.worldbank.org/doi/abs/10.1596/0-8213-5930-4

Doswell, III C. A., Brooks, H. E, & Dotzek, N. (2009). On the implementation of the enhanced Fujita scale in the USA. *Atmospheric Research*, *93*(1–3), 554–563.

Dotzek, N. (2009). Derivation of physically motivated wind speed scales. *Atmospheric Research*, *93*(1–3), 564–574.

Dunlop, S. (2008). *A dictionary of weather* (2nd ed.). Oxford University Press.

Earle, P. S., Wald, D. J., Jaiswal, K. S., Allen, T. I., Hearne, M. G., Marano, K. D., Hotovec, A. J., & Fee, J. M. (2009). *Prompt assessment of global earthquakes for response (PAGER): A system for rapidly determining the impact of earthquakes worldwide*. USGS. https://pubs.usgs.gov/of/2009/1131/

Emanuel, K. (2005). Increasing destructiveness of tropical cyclones over the past 30 years. *Nature*, *436*(4), 686–688.

England, Jr J. F., Cohn, T. A., Faber, B. A., Stedinger, J. R., Thomas, Jr W. O., Veilleux, A. G., Kiang, J. E., & Mason, Jr R. R. (2019). *Guidelines for determining flood flow frequency Bulletin 17C*. US Geological Survey. https://doi.org/10.3133/tm4B5

Fawcett, T. (2006). An introduction to ROC analysis. *Pattern Recognition Letters*, *27*(8), 861–874.

Federal Emergency Management Agency. (2020). *National Risk Index for natural hazards*. Federal Emergency Management Agency. https://www.fema.gov/flood-maps/products-tools/national-risk-index

Fedotov, S. A. (1985). Estimates of heat and pyroclast discharge by volcanic eruptions based upon the eruption cloud and steady plume observations. *Journal of Geodynamics*, *3*(3–4), 275–302.

Forebes, C., Luettich, R. A., Mattocks, C. A., & Westerink, J. J. (2010). A retrospective evaluation of the storm surge produced by Hurricane Gustav (2008): Forecast and hindcast results. *Weather and Forecasting*, *25*(6), 1577–1602.

Formetta, G., & Feyen, L. (2019). Empirical evidence of declining global vulnerability to climate-related hazards. *Global Environmental Change*, *57*, 101920.

Fry, H. T. (1967). The emergence of the Beaufort scale. *The Mariner's Mirror*, *53*(4), 311–313.

Fujita, T. T. (1971). *Proposed characterization of tornadoes and hurricanes by area and intensity*. The University of Chicago. https://ntrs.nasa.gov/search.jsp?R=19720008829

Fujita, T. T. (1981). Tornadoes and downbursts in the context of generalized planetary scales. *Journal of the Atmospheric Sciences*, *38*(8), 1511–1534.

Gardoni, P., Der Kiureghian, A., & Mosalam, K. M. (2002). Probabilistic capacity models and fragility estimates for reinforced concrete columns based on experimental observations. *Journal of Engineering Mechanics*, *128*(10), 1024–1038.

Gardoni, P., Reinschmidt, K. F., & Kumar, R. (2007). A probabilistic framework for Bayesian adaptive forecasting of project progress. *Computer-Aided Civil and Infrastructure Engineering*, *22*(3), 182–196.

Gatto, M., Bertuzzo, E., Mari, L., Miccoli, S., Carraro, L., Casagrandi, R., & Rinaldo, A. (2020). Spread and dynamics of the COVID-19 epidemic in Italy: Effects of emergency containment measures. *Proceedings of the National Academy of Sciences of the United States of America*, *117*(19), 10484–10491.

Gautam, D. (2017). Assessment of social vulnerability to natural hazards in Nepal. *Natural Hazards and Earth System Sciences*, *17*(12), 2313–2320.

Global Administrative Areas. (2018). Download GADM data. University of California. https://gadm.org/download_world.html

Government of Canada. (2017). *Wind chill – The chilling facts*. Government of Canada. http://www.ec.gc.ca/meteo-weather/default.asp?lang=n&n=5FBF816A-1#wc6

Government of Canada. (2019). *Warm season weather hazards*. Government of Canada. https://www.canada.ca/en/environment-climate-change/services/seasonal-weather-hazards/warm-season-weather-hazards.html

Grünthal, G. (1998). *European Macroseismic Scale 1998*. European Seismological Commission. http://www.bcsf.prd.fr/EMS98_Original_english.pdf

Guha-Sapir, D., Below, R., & Hoyois, P. (2020). *EM-DAT: The international disaster database*. Centre for Research on the Epidemiology of Disasters. https://www.emdat.be

Hebert, C. G., Weinzapfel, R. A., & Chambers, M. A. (2010). Hurricane Severity Index: A new way of estimating a tropical cyclone's destructive potential. In the 29th Conference on Hurricanes and Tropical Meteorology.

Hillier, J. K., & Dixon, R. S. (2020). Seasonal impact-based mapping of compound hazards. *Environmental Research Letters*, *15*(11), 114013.

Hillier, J. K., Macdonald, N., Leckebusch, G. C., & Stavrinides, A. (2015). Interactions between apparently 'primary' weather-driven hazards and their cost. *Environmental Research Letters*, *10*(10), 104003.

Hungr, O. (2018). Some methods of landslide hazard intensity mapping. In D. Cruden (Ed.), *Landslide risk assessment* (pp. 215–226). Routledge.

Hunt, E. D., Hubbard, K. G., Wilhite, D. A., Arkebauer, T. J., & Dutcher, A. L. (2009). The development and evaluation of a soil moisture index. *International Journal of Climatology*, *29*(5), 747–759.

Jackson, Jr L. E. (2013). Frequency and magnitude of events. In P. T. Bobrowsky (Ed.), *Encyclopedia of natural hazards* (pp. 359–363). Springer Science+Business Media.

Japan Meteorological Agency. (2019). *Tables explaining the JMA Seismic Intensity Scale*. Japan Meteorological Agency. http://www.jma.go.jp/jma/en/Activities/inttable.html

Kameshwar, S., & Padgett, J. E. (2014). Multi-hazard risk assessment of highway bridges subjected to earthquake and hurricane hazards. *Engineering Structures*, *78*, 154–166.

Kanamori, H. (1977). The energy release in great earthquakes. *Journal of Geophysical Research*, *82*(20), 2981–2987.

Kappes, M. S., Keiler, M., von Elverfeldt, K., & Glade, T. (2012). Challenges of analyzing multi-hazard risk: A review. *Natural Hazards*, *64*(2), 1925–1958.

Katsumata, A. (1996). Comparison of magnitudes estimated by the Japan Meteorological Agency with moment magnitudes for intermediate and deep earthquakes. *Bulletin of the Seismological Society of America*, *86*(3), 832–842.

Keeley, J. E. (2009). Fire intensity, fire severity and burn severity: A brief review and suggested usage. *International Journal of Wildland Fire*, *18*(1), 116–126.

King, G., & Zeng, L. (2001). Logistic regression in rare events data. *Political Analysis*, *9*(2), 137–163.

Koks, E. E., Rozenberg, J., Zorn, C., Tariverdi, M., Vousdoukas, M., Fraser, S. A., Hall, J. W., & Hallegatte, S. (2019). A global multi-hazard risk analysis of road and railway infrastructure assets. *Nature Communications*, *10*(1), 1–11.

Lekkas, E. L., Andreadakis, E., Kostaki, I., & Kapourani, E. (2013). A proposal for a new Integrated Tsunami Intensity Scale (ITIS-2012). *Bulletin of the Seismological Society of America*, *103*(2B), 1493–1502.

Lin, K. E., Lee, H., & Lin, T. (2017). How does resilience matter? An empirical verification of the relationships between resilience and vulnerability. *Natural Hazards*, *88*, 1229–1250.

Lindell, M. K., & Prater, C. S. (2003). Assessing community impacts of natural disasters. *Natural Hazards Review*, *4*(4), 176–185.

Liu, R., Chen, Y., Bormann, P., Ren, X., Hou, J., Zou, L., & Yang, H. (2006). Comparison between earthquake magnitudes determined by China seismograph network and US seismograph network (II): Surface wave magnitude. *Acta Seismologica Sinica*, *19*(1), 1–7.

Loat, R. (2010). *Risk management of natural hazards in Switzerland*. Federal Office for the Environment. https://www.sistemaprotezionecivile.it/allegati/1149_Svizzera_Risk_Management.pdf

Lombardo, F. T. (2012). Improved extreme wind speed estimation for wind engineering applications. *Journal of Wind Engineering and Industrial Aerodynamics*, *104–106*, 278–284.

Lombardo, F. T., & Ayyub, B. M. (2015). Analysis of Washington, DC, wind and temperature extremes with examination of climate change for engineering applications. *ASCE-ASME Journal of Risk and Uncertainty in Engineering Systems, Part A: Civil Engineering*, *1*(1), 04014005.

Lombardo, F. T., Sinh, H. N., Letchford, C., & Rosowsky, D. V. (2014). Assessing the joint wind and temperature hazard for the United States. *In Structures Congress*, 1371–1382.

Maienschein, J. L. (2002). Estimating equivalency of explosives through a thermochemical approach. In the 12th International Conference Symposium, San Diego, CA, August 11—16. USDEA.

Mayo, T., & Lin, N. (2019). The effect of the surface wind field representation in the operational storm surge model of the National Hurricane Center. *Atmosphere*, *10*(4), 193.

McEntire, D. (2012). Understanding and reducing vulnerability: From the approach of liabilities and capabilities. *Disaster Prevention and Management*, *21*(2), 206–225.

McEntire, D. A., Fuller, C., Johnston, C. W., & Weber, R. (2002). A comparison of disaster paradigms: The search for a holistic policy guide. *Public Administration Review*, *62*(3), 267–281.

McKee, T. B., Doesken, N. J., & Kleist, J. (1993). The relationship of drought frequency and duration to time scales. In the 8th Conference on Applied Climatology, January 17–22, Anaheim, CA.

Meaden, G. T., Kochev, S., Kolendowicz, L., Kosa–Kiss, A., Marcinoniene, I., Sioutas, M., Tooming, H., & Tyrrell, J. (2007). Comparing the theoretical versions of the Beaufort scale, the T-scale and the Fujita scale. *Atmospheric Research*, *83*(2–4), 446–449.

Met Office. (2019). *Wind chill factor*. Met Office. https://www.metoffice.gov.uk/weather/learn-about/weather/types-of-weather/wind/wind-chill-factor

Metropolis, N., & Ulam, S. (1949). The Monte Carlo method. *Journal of the American Statistical Association*, *44*(247), 335–341.

Mileti, D. S., & Peek, L. (2000). The social psychology of public response to warnings of a nuclear power plant accident. *Journal of Hazardous Materials*, *75*(2–3), 181–194.

Mishra, A. K., & Singh, V. P. (2010). A review of drought concepts. *Journal of Hydrology*, *391*(1–2), 202–216.

Morrow, B. H. (1999). Identifying and mapping community vulnerability. *Disasters*, *23*(1), 1–18.

Mudd, L., Rosowsky, D., Letchford, C., & Lombardo, F. (2017). Joint probabilistic wind–rainfall model for tropical cyclone hazard characterization. *Journal of Structural Engineering*, *143*(3), 04016195.

Murphy, C. (2010). *A moral theory of political reconciliation*. Cambridge University Press.

Murphy, C. (2017). *The conceptual foundations of transitional justice*. Cambridge University Press.

Murphy, C. (2020a). Religion & transitional justice. *Daedalus*, *149*(3), 185–200.

Murphy, C. (2020b). III – On principled compromise: When does a process of transitional justice qualify as just? *Proceedings of the Aristotelian Society*, *120*(1), 47–70.

Murphy, C., & Gardoni, P. (2006). The role of society in engineering risk analysis: A capabilities-based approach. *Risk Analysis*, *26*(4), 1073–1083.

Murphy, C., & Gardoni, P. (2008). The acceptability and the tolerability of societal risks: A capabilities-based approach. *Science and Engineering Ethics*, *14*(1), 77–92.

Murphy, C., & Gardoni, P. (2010). Assessing capability instead of achieved functionings in risk analysis. *Journal of Risk Research*, *13*(2), 137–147.

Murphy, C., & Gardoni, P. (2011). Evaluating the source of the risks associated with natural events. *Res Publica*, *17*(2), 125–140.

Murty, T. S., & Loomis, H. G. (1980). A new objective tsunami magnitude scale. *Marine Geodesy*, *4*(3), 267–282.

National Centers for Environmental Information. (2018). *NCEI/WDS global significant earthquake database, 2150 BC to present*. National Centers for Environmental Information. https://www.ncei.noaa.gov/access/metadata/landingpage/bin/iso?id=gov.noaa.ngdc.mgg.hazards:G012153

National Disaster Management Authority. (2008). *Guidelines on management of cyclones*. Government of India, Available at https://ndma.gov.in/Governance/Guidelines

National Hurricane Center, & Central Pacific Hurricane Center. (2019). Saffir–Simpson hurricane wind scale. https://www.nhc.noaa.gov/aboutsshws.php

National Oceanic and Atmospheric Administration. (2020). *Historical hurricane tracks*. https://coast.noaa.gov/hurricanes/#map=4/32/-80

National Weather Service. (2019a). *Heat index.* National Oceanic and Atmospheric Administration. https://www.weather.gov/safety/heat-index

National Weather Service. (2019b). *Wind chill chart*. National Oceanic and Atmospheric Administration. https://www.weather.gov/safety/cold-wind-chill-chart

Newhall, C. G., & Self, S. (1982). The volcanic explosivity index (VEI): An estimate of explosive magnitude for historical volcanism. *Journal of Geophysical Research*, *87*(C2), 1231–1238.

Nocera, F., & Gardoni, P. (2019). A ground-up approach to estimate the likelihood of business interruption. *International Journal of Disaster Risk Reduction*, *41*, 101314.

Open Source Seismic Hazard Analysis. (2010). *Intensity measure (IM)*. https://opensha.org/Glossary#intensity-measure-im

Osczevski, R., & Bluestein, M. (2005). The new wind chill equivalent temperature chart. *Bulletin of the American Meteorological Society*, *86*(10), 1453–1458.

Owens, E. H. (1982). Sea conditions. In M. L. Schwartz (Ed.), *Beaches and coastal geology* (p. 722). Springer.

Pallister, J., Wessels, R., Griswold, J., McCausland, W., Kartadinata, N., Gunawan, H., Budianto, A., & Primulyana, S. (2019). Monitoring, forecasting collapse events, and mapping pyroclastic deposits at Sinabung volcano with satellite imagery. *Journal of Volcanology and Geothermal Research*, *382*, 149–163.

Palmer, W. C. (1965). *Meteorological drought*. US Department of Commerce. https://www.ncdc.noaa.gov/temp-and-precip/drought/docs/palmer.pdf

Palmer, W. C. (1968). Keeping track of crop moisture conditions, nationwide: The new crop moisture index. *Weatherwise*, *21*(4), 156–161.

Paprotny, D., Sebastian, A., Morales-Nápoles, O., & Jonkman, S. N. (2018). Trends in flood losses in Europe over the past 150 years. *Nature Communications*, *9*(1), 1985.

Pelling, M. (2003). *The vulnerability of cities: Natural disasters and social resilience*. Earthscan.

Potter, S. (2007). Fine-tuning Fujita: After 35 years, a new scale for rating tornadoes takes effect. *Weatherwise*, *62*(2), 64–71.

Powell, M. D., & Reinhold, T. A. (2007). Tropical cyclone destructive potential by integrated kinetic energy. *Bulletin of the American Meteorological Society*, *88*(4), 513–526.

Pyle, D. M. (1995). Mass and energy budgets of explosive volcanic eruptions. *Geophysical Research Letters*, *22*(5), 563–566.

Python Software Foundation. (2020). Python 3.7.8. Python Software Foundation. https://www.python.org

Quarantelli, E. L. (1984). Perceptions and reactions to emergency warnings of sudden hazards. *Ekistics*, *51*(309), 511–515.

Rautian, T. G., Khalturin, V. I., Fujita, K., Mackey, K. G., & Kendall, A. D. (2007). Origins and methodology of the Russian Energy K-Class System and its relationship to magnitude scales. *Seismological Research Letters*, *78*(6), 579–590.

Reed, C., Biggerstaff, M., Finelli, L., Koonin, L. M., Beauvais, D., Uzicanin, A., Plumer, A., Bresee, J., Redd, S. C., & Jernigan, D. B. (2013). Novel framework for assessing epidemiologic effects of influenza epidemics and pandemics. *Emerging Infectious Diseases*, *19*(1), 85–91.

Ribot, J. (2014). Cause and response: Vulnerability and climate in the Anthropocene. *The Journal of Peasant Studies*, *41*(5), 667–705.

Richter, C. F. (1935). An instrumental earthquake magnitude scale. *Bulletin of the Seismological Society of America*, *25*(1), 1–32.

Rivera, F. I., & Kapucu, N. (2015). *Disaster vulnerability, hazards and resilience: Perspectives from Florida*. Springer International.

Rodríguez, H., Quarantelli, E. L., & Dynes, R. R. (2007). *Handbook of disaster research*. Springer Science+Business Media.

Roos, R., & Schnirring, L. (2007). *HHS ties pandemic mitigation advice to severity*. Center for Infectious Disease Research and Policy. http://www.cidrap.umn.edu/news-perspective/2007/02/hhs-ties-pandemic-mitigation-advice-severity

Rossi, J.- L., Chetehouna, K., Collin, A., Moretti, B., & Balbi, J. – H. (2010). Simplified flame models and prediction of the thermal radiation emitted by a flame front in an outdoor fire. *Combustion Science and Technology*, *182*(10), 1457–1477.

Rossi, J.-L., Chatelon, F. J., & Marcelli, T. (2019). Fire intensity. In S. L. Manzello (Ed), *Encyclopedia of wildfires and wildland–urban interface (WUI) fires*. Springer Nature, https://doi.org/10.1007/978-3-319-51727-8_51-1

Royal Meteorological Society. (2018). *The Beaufort Scale* Royal Meteorological Society. https://www.rmets.org/resource/beaufort-scale

Schmidt, A., Leadbetter, S., Theys, N., Carboni, E., Witham, C. S., Stevenson, J. A., Birch, C. E., Thordarson, T., Turnock, S., Barsotti, S., Delaney, L., Feng, W., Grainger, R. G., Hort, M. C., Höskuldsson, Á., Ialongo, I., Ilyinskaya, E., Jóhannsson, T., Kenny, P., … Shepherd, J. (2015). Satellite detection, long-range transport, and air quality impacts of volcanic sulfur dioxide from the 2014–2015 flood lava eruption at Bárðarbunga (Iceland). *Journal of Geophysical Research: Atmospheres*, *120*(18), 9739–9757.

Serva, L., Vittori, E., Comerci, V., Esposito, E., Guerrieri, L., Michetti, A. M., Mohammadioun, B., Mohammadioun, G. C., Porfido, S., & Tatevossian, R. E. (2016). Earthquake hazard and the Environmental Seismic Intensity (ESI) scale. *Pure and Applied Geophysics*, *173*(5), 1479–1515.

Shafer, B. A., & Dezman, L. E. (1982). Development of a surface water supply index (SWSI) to assess the severity of drought conditions in snowpack runoff areas. In the 50th Annual Western Snow Conference. https://westernsnowconference.org/node/932

Shafiei Shiva, J., Chandler, D. G., & Kunkel, K. E. (2019). Localized changes in heat wave properties across the United States. *Earth's Future*, *7*(3), 300–319.

Shukla, S., & Wood, A. W. (2008). Use of a standardized runoff index for characterizing hydrologic drought. *Geophysical Research Letters*, *35*(2), L02405.

Shuto, N. (1993). Tsunami intensity and disasters. In S. Tinti (Ed.), *Tsunamis in the world* (pp. 197–216). Springer Science+Business Media.

Simpson, R. H., & Saffir, H. (1974). The hurricane Disaster-Potential Scale. *Weatherwise*, *27*(4), 169–186.

Singh, A., Kanungo, D. P., & Pal, S. (2019). A modified approach for semi-quantitative estimation of physical vulnerability of buildings exposed to different landslide intensity scenarios. *Georisk: Assessment of Management of Risk for Engineered Systems and Geohazards*, *13*(1), 66–81.

Smythe, D. (2011). *An objective nuclear accident magnitude scale for quantification of severe and catastrophic events*. Physics Today: Points of view. http://www.davidsmythe.org/professional/pdf/NAMS%20Points%20of%20View.pdf

Space Weather Prediction Center. (2011). *NOAA space weather scales*. National Oceanic and Atmospheric Administration. https://www.swpc.noaa.gov/sites/default/files/images/NOAAscales.pdf

Space Weather Prediction Center. (2019). *Solar flares (radio blackouts)*. National Oceanic and Atmospheric Administration. https://www.swpc.noaa.gov/phenomena/solar-flares-radio-blackouts

spia-index.com. (2019). What is the Sperry–Piltz ice accumulation index? https://www.spia-index.com

Steadman, R. G. (1979). The assessment of sultriness. Part I: A temperature–humidity index based on human physiology and clothing science. *Journal of Applied Meteorology*, *18*(7), 861–873.

Sutley, E. J., van de Lindt, J. W., & Peek, L. (2017). Multihazard analysis: Integrated engineering and social science approach. *Journal of Structural Engineering*, *143*(9), 04017107.

Tanyaş, H., Allstadt, K. E., & van Westen, C. J. (2018). An updated method for estimating landslide–event magnitude. *Earth Surface Processes and Landforms*, *43*(9), 1836–1847.

Tate, E. (2012). Social vulnerability indices: A comparative assessment using uncertainty and sensitivity analysis. *Natural Hazards*, *63*(2), 325–347.

The Tornado and Storm Research Organisation. (2021). The TORRO hailstorm intensity scale. https://www.torro.org.uk/research/hail/hscale

Turner, B. L., Kasperson, R. E., Matson, P. A., McCarthy, J. J., Corell, R. W., Christensen, L., Eckley, N., Kasperson, J. X., Luers, A., Martello, M. L., Polsky, C., Pulsipher, A., & Schiller, A. (2003). A framework for vulnerability analysis in sustainability science. *Proceedings of the National Academy of Sciences*, *100*(14), 8074–8079.

Typhoon Committee. (2018). *Tropical cyclone classification*. Typhoon Committee. http://www.typhooncommittee.org/tropical-cyclone-classification

US Geological Survey. (2018). *Search earthquake catalog*. US Geological Survey. https://earthquake.usgs.gov/earthquakes/search

van de Lindt, J. W., Peacock, W. G., Mitrani-Reiser, J., Rosenheim, N., Deniz, D., Dillard, M., Tomiczek, T., Koliou, M., Graettinger, A., Crawford, P. S., Harrison, K., Barbosa, A., Tobin, J., Helgeson, J., Peek, L., Memari, M., Sutley, E. J., Hamideh, S., Gu, D., … Fung, J. (2020). Community resilience-focused technical investigation of the 2016 Lumberton, North Carolina, flood: An interdisciplinary approach. *Natural Hazards Review*, *21*(3), 04020029.

Wald, D. J., Worden, B. C., Quitoriano, V., & Pankow, K. L. (2006). *ShakeMap manual: Technical manual, users guide, and software guide*. US Geological Survey, Available at https://doi.org/10.3133/tm12A1

Walker, G. P. L. (1973). Explosive volcanic eruptions – A new classification scheme. *Geologische Rundschau*, *62*(2), 431–446.

Wang, H. (2020). Estimating flood risk impact on farmland values using boundary discontinuity: Evidence from Lancaster County, Pennsylvania. *Risk Analysis*, Available at https://doi.org/10.1111/risa.13623

Wang, Y. V. (2020). Empirical local hazard models for bolide explosions. *Natural Hazards Review*, *21*(4), 04020037.

Wang, Y. V., Tabandeh, A., Gardoni, P., Hurt, T. M., Hartman, E. R., & Myers, N. R. (2016). *Assessing socioeconomic impacts of cascading infrastructure disruptions using the capability approach*. US Army Corps of Engineers Engineer Research and Development Center. https://apps.dtic.mil/sti/citations/AD1016582

Wang, Y. V., Gardoni, P., Murphy, C., & Guerrier, S. (2019). Predicting fatality rates due to earthquakes accounting for community vulnerability. *Earthquake Spectra*, *35*(2), 513–536.

Wang, Y. V., Gardoni, P., Murphy, C., & Guerrier, S. (2020). Worldwide predictions of earthquake casualty rates with seismic intensity measure and socioeconomic data: A fragility-based formulation. *Natural Hazards Review*, *21*(2), 04020001.

Wang, Y. V., Gardoni, P., Murphy, C., & Guerrier, S. (2021). Empirical predictive modeling approach to quantifying social vulnerability to natural hazards. *Annals of the American Association of Geographers*, *111*(5), 1559–1583.

Wang, Y. V., & Sebastian, A. (2021a). Community flood vulnerability and risk assessment: An empirical predictive modelling approach. *Journal of Flood Risk Management*, *14*(3), e12739.

Wang, Y. V., & Sebastian, A. (2021b). Equivalent hazard magnitude scale. Natural Hazards and Earth System Sciences Discussion. [Preprint]. https://doi.org/10.5194/nhess-2021-87

Wheatley, S., Sovacool, B., & Sornette, D. (2017). Of disasters and dragon kings: A statistical analysis of nuclear power incidents and accidents. *Risk Analysis*, *37*(1), 99–115.

Wisner, B., Blaikie, P., Cannon, T., & Davis, I. (2004). *At risk: Natural hazards, people's vulnerability and disaster* (2nd Ed.). Routledge.

Wood, H. O., & Neumann, F. (1931). Modified Mercalli intensity scale of 1931. *Bulletin of the Seismological Society of America*, *21*(4), 277–283.

World Meteorological Organization. (2016). *Tropical cyclone operational plan for the South–West Indian Ocean*. World Meteorological Organization. https://library.wmo.int/doc_num.php?explnum_id=4031

Xu, W., Ming, X., Ma, Y., Zhang, X., Shi, P., Zhuo, L., & Lu, B. (2019). Quantitative multi-hazard risk assessment of crop loss in the Yangtze River Delta region of China. *Sustainability*, *11*(3), 922.

Zeff, H., Characklis, G. W., & Thurman, W. (2020). How do price surcharges impact water utility financial incentives to pursue alternative supplies during drought? *Journal of Water Resources Planning and Management*, *146*(6), 04020042.

How to cite this article: Wang, Y. V., & Sebastian, A. (2022). Murphy Scale: A locational equivalent intensity scale for hazard events. *Risk Analysis*, 1–19. https://doi.org/10.1111/risa.13933